

RESEARCH ON OXYGEN RECOVERY SYSTEMS
FOR USE IN SPACE CAPSULES

Progress Report for the Period
February 1972-January 1973

by

J. R. Selman, R. K. Steunenberg,
and E. J. Cairns

February 1973

(NASA-CR-114573) RESEARCH ON OXYGEN
RECOVERY SYSTEMS FOR USE IN SPACE
CAPSULES Progress Report, Feb. 1972 -
Jan. 1973 (Argonne National Lab., Ill.)
52 p HC \$4.75

N73-25130

CSCL 06K

G3/05

Unclas
07082

Distribution of this report is provided in the
interest of information exchange. Responsi-
bility for the contents resides in the author
or organization that prepared it.

This report is also known as ANL-8018

Prepared under NASA Order A-70738A according
to an Agreement between the
National Aeronautics and Space Administration
and the U. S. Atomic Energy Commission

by

Chemical Engineering Division
ARGONNE NATIONAL LABORATORY
9700 South Cass Avenue
Argonne, Illinois 60439

for

AMES RESEARCH CENTER
NATIONAL AERONAUTICS AND SPACE ADMINISTRATION



RESEARCH ON OXYGEN RECOVERY SYSTEMS
FOR USE IN SPACE CAPSULES

Progress Report for the Period
February 1972-January 1973

by

J. R. Selman, R. K. Steunenberg,
and E. J. Cairns

February 1973

Distribution of this report is provided in the
interest of information exchange. Responsi-
bility for the contents resides in the author
or organization that prepared it.

This report is also known as ANL-8018

Prepared under NASA Order A-70738A according
to an Agreement between the
National Aeronautics and Space Administration
and the U. S. Atomic Energy Commission

by

Chemical Engineering Division
ARGONNE NATIONAL LABORATORY
9700 South Cass Avenue
Argonne, Illinois 60439

for

AMES RESEARCH CENTER
NATIONAL AERONAUTICS AND SPACE ADMINISTRATION

TABLE OF CONTENTS

	<u>Page</u>
SUMMARY.	1
I. INTRODUCTION	3
A. Electrochemical Cell Reactions	3
B. Differences Between the Present Design and That of United Aircraft	6
C. Flow Diagram of the Proposed System.	9
II. EXPERIMENTAL	11
A. Electrochemical Cell	11
1. Design and Materials	11
2. Electrolyte.	17
B. Gas Supply-System and Furnace.	22
1. Glovebox Atmosphere.	22
2. Furnace.	22
3. Gas-Supply System.	22
C. Gas Analysis	24
D. Experimental Approach.	24
1. Stepped-Potential Scanning	26
2. Optimization of Gas Composition.	28
3. Effect of Total Gas Flow Rates	28
4. Constant-Current Operation	28
E. Initial Experiments.	28
CONCLUSIONS AND STATUS	32
APPENDIX A: THERMODYNAMIC DATA ON ACETYLIDES	33
APPENDIX B: GAS SUPPLY SYSTEM.	34
APPENDIX C: GAS ANALYSIS OF SYNTHETIC SAMPLES.	37

Table of Contents (cont.)

	<u>Page</u>
APPENDIX D: DIMENSIONAL DRAWINGS OF ELECTRODES.	42
REFERENCES.	46

LIST OF FIGURES

<u>Number</u>	<u>Title</u>	<u>Page</u>
1	Over-all Reactant Flows, Relative to 1 mole CO ₂ and 1 mole H ₂ O.	5
2	Reactant Flows in the Cathode When Excess H ₂ O Feed is 10%.	7
3	Schematic Concentration Profiles, Current Density and Potential Distribution in the Cathode	8
4	Flow Diagram of Regeneration Scheme	10
5	Cross Section of the Electrochemical Cell Inside the Furnace Well.	12
6	Cathode and Anode (Submerged Parts)	13
7	Construction of Cathode Holder, Plate, and Cap.	15
8	Construction of Baffle Inside Cathode	16
9a	Cathode With Inner Tube Partially Exposed	20
9b	Inner and Outer Tubes of the Cathode, Disassembled.	20
10a	Lower End of the Anode Assembly (Inner Tube Partially Exposed).	21
10b	Full Anode Assembly (Inner Tube Partially Exposed).	21
11	Schematic Flow Diagram of Gas-Supply System	23
12	Design of Capillary Flowmeter (Schematic)	25
13	Polarization Curve.	30

APPENDICES

B.1	Schematic Flow Diagram of the Gas Supply System	35
D.1a	Cathode, Upper Part (Vertical Section).	43
D.1b	Cathode, Lower Part (Vertical Section and Horizontal Section Through Cathode Holder)	44
D.2	Anode (Vertical Section).	45

LIST OF TABLES

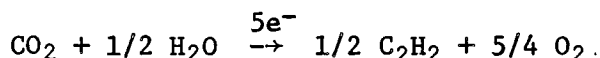
<u>Number</u>	<u>Title</u>	<u>Page</u>
I	Materials Available for Porous Cathode Plates	18
II	Metals in Order of Decreasing Hydrogen Overvoltage. . .	19
III	Cell Potentials for Reactions (9)-(15).	27

APPENDICES

A.I	Standard Enthalpy and Gibbs Energy of Formation of Alkaline and Alkaline Earth Acetylides (in kcal/mole) .	33
B.I	Estimated Hold-up Volumes	36
C.I	Analysis of Anode Gas Sample.	38
C.II	Analysis of Cathode Gas Sample, Using Syringe Sampling.	38
C.III	Analysis of Second Cathode Gas Sample, Using 1-ml Loop .	40
C.IV	Second Virial Coefficients and Compressibility Factors of Reactant and Product Component Gases	40
C.V	Peak Height Response for Pure Components and For Mixed Gas Samples	41

SUMMARY

This program consists of research studies on an improved electrochemical process for the recovery of oxygen from the atmospheres of manned space capsules. The objective of the proposed system is to recover the oxygen from CO_2 with high efficiency and to recover the additional amount of oxygen from water that is required to provide a total oxygen makeup stream of about 2.0 lb/man-day. The carbon from the CO_2 must be converted into a readily disposable or usable form. A particularly desirable reaction would be the overall reaction



The Hamilton Standard Division of the United Aircraft Corp. has investigated a system employing a high-temperature electrochemical cell, which has a LiCl-SrCl_2 electrolyte containing small additions of Li_2O and Li_2CO_3 . The CO_2 and H_2O in the cabin atmosphere are both fed to the anode of the cell, where they react with the O^- in the electrolyte to form CO_3^- and OH^- , respectively. The CO_3^- is reduced electrochemically at the cathode to C_2^- , which reacts with OH^- to form gaseous C_2H_2 and O^- . The O^- ions are oxidized at the anode to form oxygen, which is recycled to the cabin atmosphere. One practical difficulty with this scheme is that operation of the cathode at the potential required to form C_2^- ions produces concentration gradients in the electrolyte, causing the $\text{C}_2^- + \text{OH}^-$ reaction zone to move away from the cathode into the bulk electrolyte. The C_2H_2 product of the reaction forms bubbles in the electrolyte which tend to decrease the efficiency of the cell, and special provisions are required to recover the gaseous C_2H_2 . Another difficulty is that some carbon is formed at the cathode because of the low concentration of OH^- ions available to react with the C_2^- ions.

In the current program, certain modifications of this system are being investigated. The main difference in the present scheme is that the CO_2 is fed to the anode and H_2O is fed to the cathode. The intent of this change was to adjust the conditions in such a way that the formation of C_2H_2 occurs within the porous cathode, from which it can escape readily by gaseous diffusion through the pores, thereby avoiding the problem of separating it from the electrolyte. It was also considered possible that the tendency to form carbon would be decreased by this mode of operation.

The cathode and anode designed and fabricated for the experiments are essentially concentric tubes extending down a furnace well into a beaker containing the molten electrolyte. The cathode reaction takes place in a porous metal disk inserted into the end of a stainless steel (Type 347) tube by means of a bayonet fitting. H_2O vapor in argon carrier gas is led down the cathode holder tube and contacts the electrolyte inside the porous cathode disk where the cathode reaction takes place. Together with the gaseous reaction products, it exits through the concentric, inner, cathode tube. CO_2 in helium carrier gas is led down the inner anode tube and sparged into the electrolyte but contained within the anode outer tube. It exits, together with the oxygen produced by the anode reaction, through the annular space between inner and outer tube.

The anode parts in contact with the electrolyte were fabricated from gold-40 wt % palladium alloy, the remainder of stainless steel, Type 347 or 304. The cathode, including those parts in contact with the electrolyte, was fabricated of stainless steel, Type 347.

The gas supply system was designed for accurate flow control and measurement at pressures above atmospheric and flow rates in the range of 0.1-100 ml/min. Since containment of the reactant and product gases can be inferred only from material balances, the pressure tightness of the system was given special attention. For the same reason, the accuracy of the gas-chromatographic analyses of component fractions was checked and found to be approximately 3-5%.

In the initial experiments a stainless steel (Type 347) disk of uniform porosity was used as the cathode disk. The electrolyte was LiCl-KCl eutectic with small additions of Li_2O , Li_2CO_3 , and LiOH at approximately 430°C .

Results obtained by stepwise increasing the cell voltage, while maintaining constant-feed gas flow rates, indicate a current plateau between 1.1 and 1.3 V, probably due to hydrogen formation, and a plateau between 1.3 and 1.6 V, which is tentatively assigned to the reduction of carbonate ions. In this potential range, the current continues to decrease and reaches a fairly steady qualitative test for acetylene because of leaks in the exit side of the cathode gas line. This problem is being corrected by repairing the leaks and shortening the gas train to reduce the flow resistance so that operation at less than atmospheric pressure will not be necessary.

Stainless steel parts in contact with the electrolyte assume a potential of approximately -100 mV with respect to the grounded gold beaker. After 100 hr at open circuit, these parts show corrosion (grain-boundary attack and pitting) just above the electrolyte level. Although stainless steel is being used for reasons of economy in the design stages of the cell, corrosion-resistant materials, such as rhodium in the cathode and gold in the anode, could be used in a practical application.

Efforts are now being directed toward positive identification of the product gases at the 1.3-1.6 V current plateau.

I. INTRODUCTION

This program, which was initiated on January 24, 1972, consists of research studies on an improved electrochemical process for the recovery of oxygen from the atmospheres of manned space capsules. The production rates of CO_2 and H_2O are assumed to be 2.20 and 3.55 lb/man-day, respectively, and the consumption of oxygen between 1.84 and 2.53 lb/man-day, depending on the amount lost by cabin leakage. The total pressure in the cabin is to be 10 psia, consisting of the following partial pressures (in psia): O_2 , 3.16; N_2 , 6.62; CO_2 , 0.06; H_2O , 0.16. The objective of the proposed system is to recover the oxygen from CO_2 with high efficiency and to recover an additional amount of oxygen from water. The latter is required to provide a total oxygen-makeup stream of about 2.0 lb/man-day. The carbon from the CO_2 must be converted into a readily disposable or usable form. Conversion of the carbon into a hydrocarbon, using the hydrogen by-product of the oxygen production from water, requires that the hydrogen:carbon atom ratio of the hydrocarbon be close to unity. For this reason, acetylene appears to be a desirable product.

The Hamilton Standard Division of the United Aircraft Corp.¹ has proposed a cabin atmosphere regeneration system employing a high-temperature electrochemical cell, which has a molten electrolyte consisting of LiCl and SrCl_2 with small additions of Li_2O and Li_2CO_3 . The CO_2 and H_2O in the cabin atmosphere are both fed to the anode of the cell, where they react with the O^\ominus in the electrolyte to form CO_3^\ominus and OH^\ominus ions, respectively. The CO_3^\ominus diffuses through the bulk electrolyte to the cathode, where it is reduced electrochemically to C_2^\ominus ions, which react with OH^\ominus to form gaseous C_2H_2 and O^\ominus ions. The O^\ominus ions are oxidized electrochemically at the anode to form gaseous oxygen, which is recycled to the cabin atmosphere. Although this scheme is attractive in principle, one practical difficulty is that operation of the cathode at the potential required to form C_2^\ominus ions produces concentration gradients in the electrolyte, causing the $\text{C}_2^\ominus + \text{OH}^\ominus$ reaction zone to move away from the cathode into the bulk electrolyte. The C_2H_2 produced by the reaction forms bubbles in the electrolyte, which tends to decrease the efficiency of the cell, and special provisions are required to recover the gaseous C_2H_2 . Another difficulty is that some carbon is formed at the cathode because of the low concentration of OH^\ominus ions available to react with the C_2^\ominus ions.

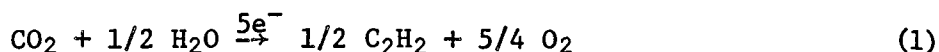
In the current program, certain modifications of this system are to be investigated. The main difference in the present scheme is that the CO_2 is fed to the anode and H_2O is fed to the cathode. The intent of this change is to adjust the conditions in such a way that the formation of C_2H_2 occurs within the porous cathode, from which it can escape readily by gaseous diffusion through the pores, thereby avoiding the problem of separating it from the electrolyte. It is also possible that the tendency to form carbon will be decreased by this mode of operation.

A. Electrochemical Cell Reactions

In the following discussion, a number of chemical and electrochemical reactions are shown to illustrate the operation of the proposed system. It should be recognized that the mechanisms of these reactions are not understood

in detail and that other side reactions or competing reactions may be involved. A better understanding of the chemistry and electrochemistry involved in the operation of this type of cell is a major objective of the research program.

The cell design is based upon the oxygen requirement of 2.00 lb/man-day, which, in principle, can be met fully by the following reaction of the available CO₂ (2.20 lb/man-day) with H₂O:



The amount of H₂O needed for this reaction is 0.45 lb/man-day. To carry out reaction (1) by this process, the reduction of carbonate to acetylide must be made to occur simultaneously with hydrolysis of the acetylide to form C₂H₂.

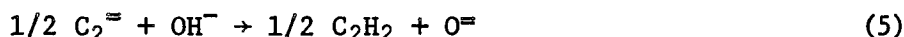
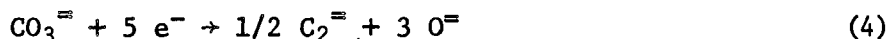
In the proposed cell the CO₂ is fed into the porous anode and the H₂O into the porous cathode (Fig. 1). At the anode, the CO₂ reacts with some O⁼ ions in the electrolyte to form CO₃⁼ ions:



which are transported by diffusion through the bulk electrolyte to the cathode. At the cathode, the H₂O reacts with O⁼ ions in the electrolyte to form OH⁻ ions:



The thickness, porosity, pore size, and material used in the cathode are selected so that the reduction of CO₃⁼ and the formation of C₂H₂ take place within the cathode structure:



The cathode material is to have a dual porosity, that is, micropores filled with electrolyte and macropores filled with gas. The macropore structure provides a path for the transport of the C₂H₂ product out of the cathode. The O⁼ ions produced by reactions (4) and (5) are partially consumed by the formation of OH⁻ ions by reaction (3). The remaining O⁼ ions are transported by diffusion and migration through the electrolyte toward the anode, where some participate in reaction (2), but most are oxidized electrochemically to form oxygen gas:



To satisfy the requirements of the system, the mole ratio of the H₂O and CO₂ fed to the cathode and anode, respectively, need not be greater than 1:2. However, the cathode must be maintained at the acetylide-forming potential, which is expected to result in the formation of some hydrogen through the electrochemical reduction of a fraction of the OH⁻ ions produced by reaction (3):



The hydrogen will diffuse out of the cathode along with the C₂H₂. The O⁼ ions from reaction (7) will increase the O⁼ ion flux through the bulk electrolyte toward the anode.

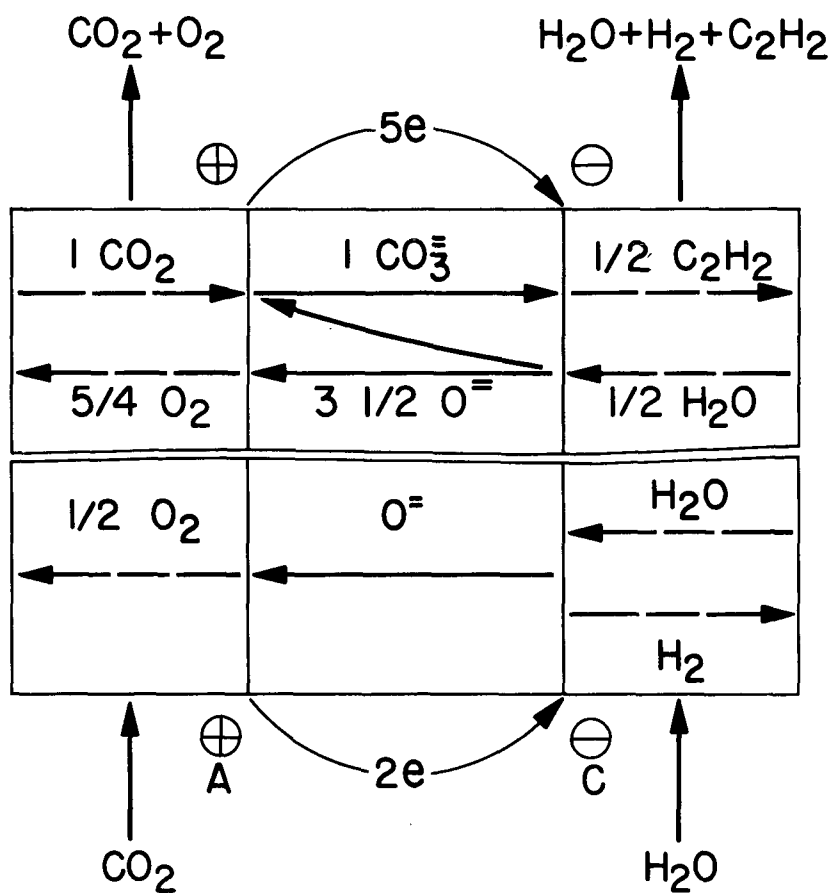


Fig. 1. Overall Reactant Flows, Relative to 1 Mol CO_2 and 1 Mol H_2O

In the cathode, it is necessary to maintain a local concentration and flux of OH^- ions sufficient to allow reaction (5) to go to completion and to minimize the rate of back-diffusion of $\text{C}_2^{=}$ ions into the bulk electrolyte. In order to maintain the required concentration and flux of OH^- ions, H_2O will be supplied in the cathode feed stream. The amount of H_2O required in the cathode feed (see Fig. 2, which shows the details of the cathode process) is taken to be 1.10 times the mole flow rate of CO_2 fed to the anode. However, this quantity cannot be estimated reliably without solving a complicated set of equations for the ionic species (OH^- , $\text{O}^{=}$, $\text{C}_2^{=}$, $\text{CO}_3^{=}$), the gaseous species (C_2H_2 , H_2O , H_2), and the ionic and electronic currents within the cathode. The distributions of the concentration, potential and current in the gas and electrolyte pores, and in the metal phase of the cathode, are shown schematically in Fig. 3. Computation of these distributions, based on estimated transport properties (diffusivities, etc.) and kinetic parameters, might be helpful in determining, for example, those conditions under which the tendency for carbon formation by the reaction



would be minimized. It must be recognized, however, that such computations would have to be based upon several assumptions and upon estimates of many thermodynamic, kinetic, and transport properties involved in this system. Experimental studies therefore are essential in order to establish the feasibility of the scheme.

B. Differences Between the Present Design and That of United Aircraft

a) In the United Aircraft system,¹ dilute CO_2 and H_2O in the cabin atmosphere are both fed to the cathode of the electrochemical cell. In the present scheme, CO_2 is fed to the anode and H_2O is fed to the cathode. The initial plan is to use essentially pure, undiluted CO_2 and H_2O from the cabin-atmosphere scrubbing system. It appears, however, that it may be possible to remove only the H_2O from the cabin atmosphere and feed it alone to the cathode of the cell, and then scrub the CO_2 by passing the dried cabin atmosphere through the anode compartment. This solution appears attractive because the use of a carrier gas, such as nitrogen or air, would probably complicate the cathode reaction by reduction of oxygen or nitrogen. Moreover, oxygen in the cathode feed gas could also cause explosive C_2H_2 -oxygen mixtures to be formed in the cathode product gas. Dilution of the combustion mixture to below the explosive limit (2.5 vol % C_2H_2 in air at room temperature) would require large amounts of carrier gas and thus cause further design problems.

b) In the United Aircraft cell, acetylide diffuses back from the cathode into the bulk electrolyte, where it is expected to react with OH^- ion, forming C_2H_2 [reaction (5)]. However, some carbon is formed in a reaction zone near the cathode. In the present design, the reaction zone is located within the cathode (Fig. 2), where the $\text{CO}_3^{=}$ ion concentration should be low so that the tendency for carbon formation by reaction (8) is minimized.

c) In the United Aircraft system, H_2O was introduced at the anode in an amount sufficient to provide the required hydrogen:carbon ratio at the cathode. In the present cell design, the H_2O is introduced at the porous

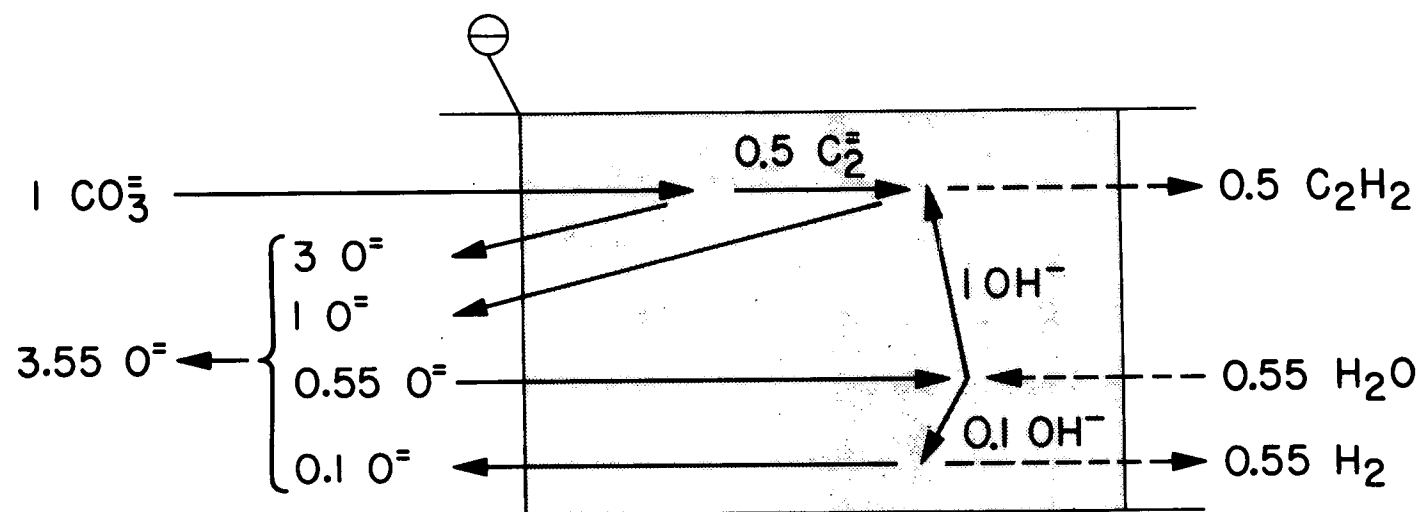


Fig. 2. Reactant Flows in the Cathode When Excess H_2O Feed is 10% (All Quantities Relative to 1 Mol of CO_2 Fed at the Anode)

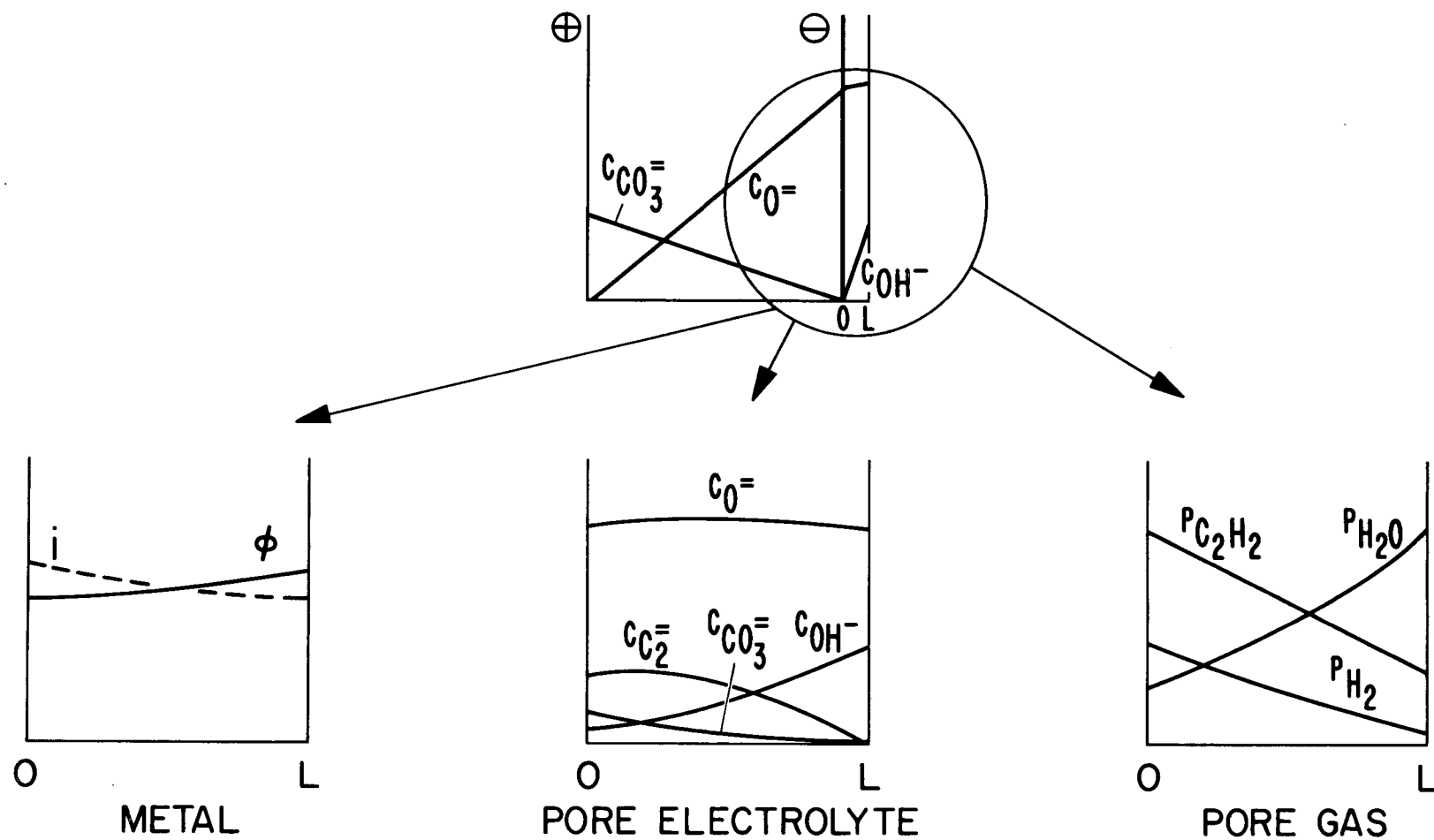


Fig. 3. Schematic Concentration Profiles, Current Density, and Potential Distribution in the Cathode (P=Partial Pressure, C=Concentration, i =Current Density, ϕ =Potential)

cathode in an amount sufficient to maintain the necessary flux of OH^- ions into the cathode where the $\text{C}_2^{=}$ ions are being produced. This is expected to result in the production of some excess hydrogen, but this reaction might be minimized by an appropriate choice of cathode structure, thickness, and material. The main advantage of this procedure is that the C_2H_2 should be produced within the cathode by reaction (5). The gaseous C_2H_2 product can then diffuse through the macropores to the cathode compartment, where it, along with any hydrogen and unreacted H_2O that are present, becomes an effluent gas stream.

d) The electrolyte that was used in the United Aircraft cell is the LiCl-SrCl_2 eutectic, with added O^- and $\text{CO}_3^{=}$, at 550°C . The electrolyte to be used initially in the present experiments is the LiCl-KCl eutectic (m.p. 352°C) with added OH^- or O^- .

C. Flow Diagram of the Proposed System

It is assumed for the present that the CO_2 and H_2O are separated from the cabin atmosphere (31.6 vol % O_2 , 66.2 vol % N_2 , 0.6 vol % CO_2 , 1.6 vol % H_2O) before they are fed to the electrochemical cell. However, as mentioned earlier, it is possible in principle to separate only the H_2O for the cathode feed and use the remaining $\text{N}_2\text{-O}_2\text{-CO}_2$ mixture as the anode feed. This scheme, however, may prove to be undesirable because of the additional equipment required to handle the problem of heat exchange between the cabin atmosphere and the electrochemical cell.

A flow diagram of the system is presented in Fig. 4. Recovery of oxygen from CO_2 with the required high efficiency probably could be accomplished best by passing the CO_2 through the anodes of several cells in series. The successive cells could be operated at decreasing current densities in order to maintain a reasonably high electrical efficiency in the last stages. It is estimated that a $\text{CO}_2\text{-O}_2$ mixture containing 95 vol % oxygen could be produced by a battery of about three cells. This mixture is returned to the cabin-atmosphere circulation system prior to the CO_2 scrubber.

Pure H_2O is fed to the cathode, where it is partially converted to a mixture of H_2 and C_2H_2 . Experimental work will be required to determine the proportion of hydrogen to be expected in this mixture. In Fig. 4 the H_2O feed rate is 10% in excess of the stoichiometric requirement for the formation of C_2H_2 . The effluent gas from the cathode is contacted with a silver-palladium diaphragm at 500°C to separate the hydrogen. The other side of the diaphragm is in contact with the effluent gas from the anode, so H_2O is formed by the catalytic combination of oxygen and hydrogen. The H_2O product is recovered from the anode effluent by means of a cold trap and reused. A cold trap is also used to recover H_2O from the cathode product, and the remaining C_2H_2 is vented. There is a possibility that a reaction between C_2H_2 and H_2O could occur on the silver-palladium surface at 500°C . If necessary, this reaction could be avoided by removing the H_2O prior to the C_2H_2 -hydrogen separation.

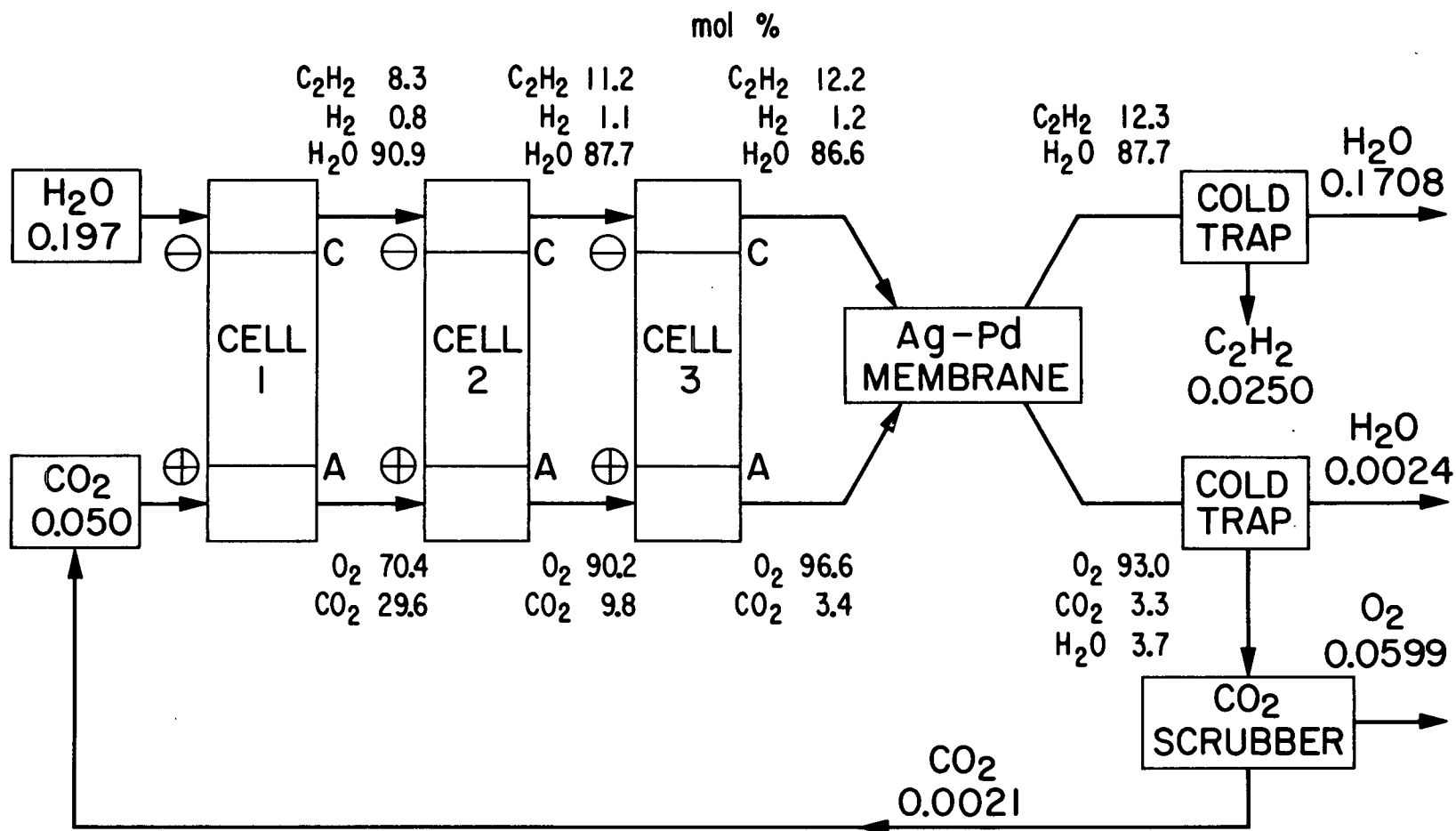


Fig. 4. Flow Diagram of Regenerative Scheme; Large Numerals Are lb-mol/man-day

II. EXPERIMENTAL

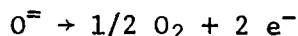
A. Electrochemical Cell

1. Design and Materials

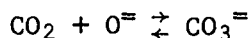
A simple electrode configuration, as shown in Fig. 5, has been selected for the initial experiments.* The cathode and the anode each are essentially two concentric tubes, 53.5 cm (21 in.) long, extending down a furnace well into a beaker containing the molten electrolyte. The electrodes are aligned in parallel by means of a baffle in the well and by the furnace lid. The furnace lid is an electrical insulator. The baffle also prevents a bottom-to-top temperature decrease in the well, since this would promote the tendency of the molten salt to creep up the electrodes and the wall of the beaker. Even under isothermal conditions carbonate or carbonate-chloride melts have a strong tendency to form films because of their high surface tension; *e.g.*, for a 10-70-20 mol % mixture of $\text{Li}_2\text{O-LiCl-Li}_2\text{CO}_3$ at 579°C , $\gamma = 154.4 \text{ dyn/cm}^2$. For the same mixture at 400°C , the value is an estimated 10 dyn/cm higher. In the present cell design, a slight top-to-bottom temperature drop is maintained by adjusting the position of the beaker with respect to the heating mantle and by inserting a heat sink under the well.

A 600-ml stainless steel beaker with a gold liner was used to contain the electrolyte. Type 347 stainless steel was used for the sparger and thermocouple sheath tubes. The sparger serves to blanket the cell continuously with inert gas, thereby preventing accumulation of explosive gases in the furnace well. If the containment of the product gases in the cathode and in the anode can be assured, routine sparging will not be necessary in the final design of the cell.

The designs of the cathode and anode are shown in cross section in Fig. 6. The anodic reaction, reaction (6),



and reaction (2),



occur at the perforated end of the inner tube, where CO_2 flowing downward comes in contact with the electrolyte. The anode current lead is a gold wire inside the inner tube, attached to a gold-wire screen inserted in the perforated end of the anode tube. The oxygen-containing product gas stream escapes through the perforations and is collected inside the annular space between the inner anode tube and the outer tube (shield). The wetted surface of the inner tube serves also as an anode for reaction (6), but at a potential slightly different from that of the gold wire, since the tube material is gold-40 wt % palladium alloy, to provide greater structural strength than that of gold itself. The

*Consideration will eventually have to be given to a cell design suitable for operation in zero gravity. For example, centrifugation might be used to maintain the necessary separation of liquid and gas phases.

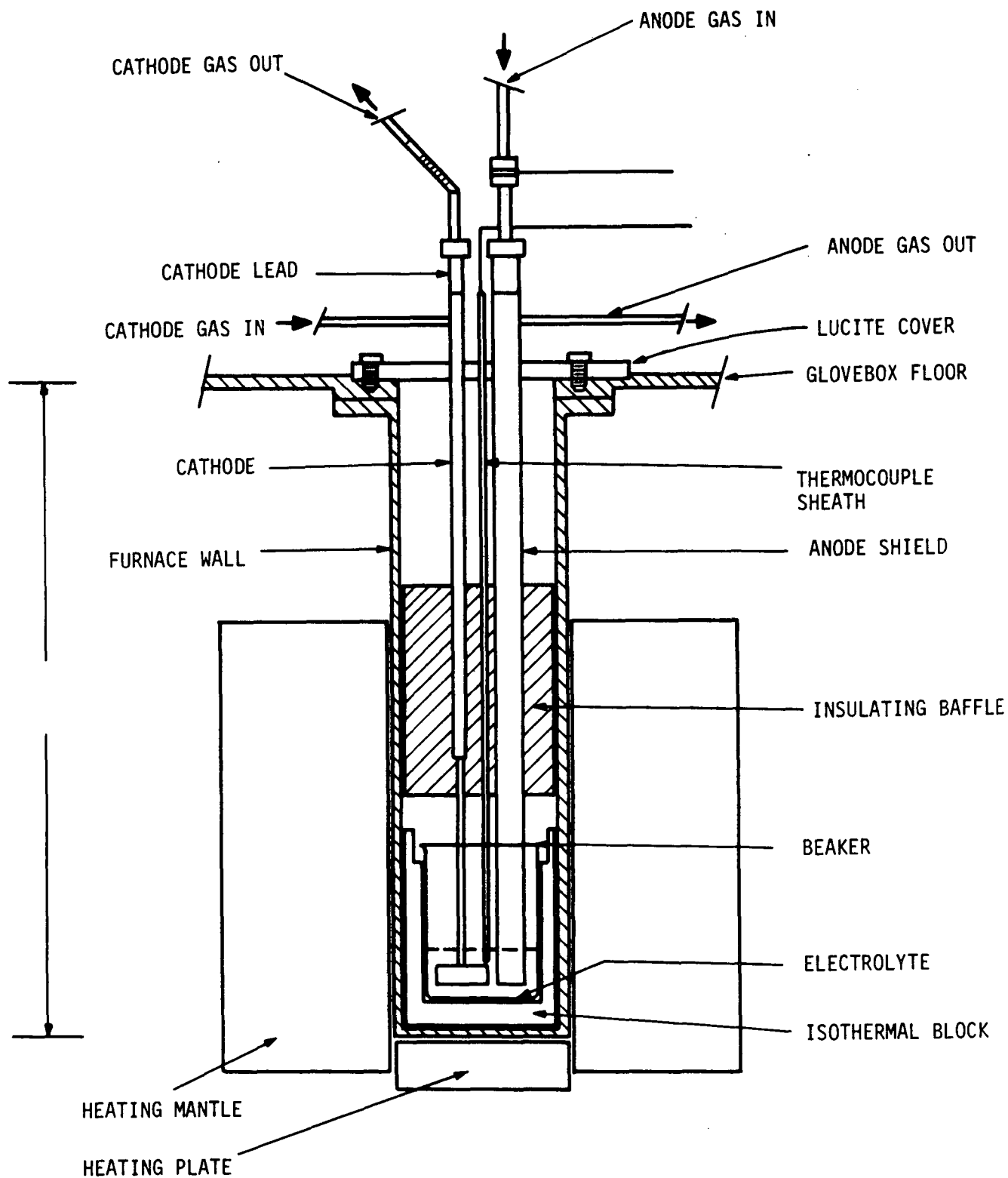


Fig. 5. Cross Section of the Electrochemical Cell
Inside the Furnace Well

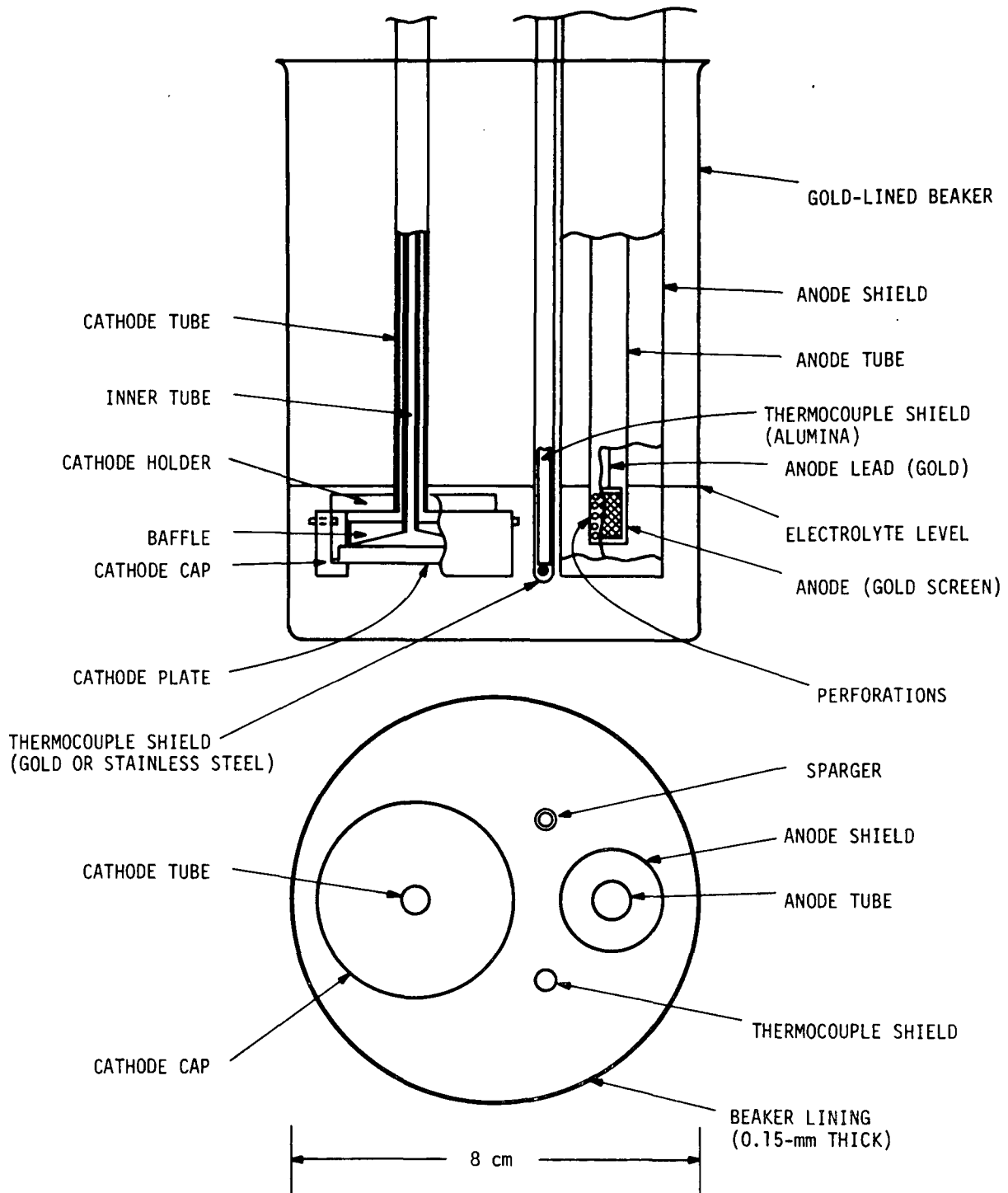


Fig. 6. Cathode and Anode (Submerged Parts)

outer tube is likewise fabricated from this alloy. It is insulated from the inner tube at its upper end by using a metal-to-glass joint.

The choice of the anode material is based upon experience with corrosion in carbonate-oxide-chloride melts as reported by United Aircraft.³ Only gold, rhodium, and iridium appear to have adequate corrosion resistance. Therefore, a gold alloy is being used for the submerged part of the anode assembly and an additional 16.5 cm (6.5 in.) above the electrolyte level. The upper part of the anode assembly is fabricated from Type 304 stainless steel.

The choice of a cathode material is also based on reported experience in carbonate-oxide-chloride melts at lithium-forming potentials.³ Rhodium and iridium appear to be the least prone to alloy formation with lithium, which would reduce the tendency to form lithium carbide at the cathode. Ideally, therefore, the cathode reaction should take place within a disk of, for example, porous rhodium. The sintered disk could be 0.3 cm thick and should consist of two layers, one formed from powder of less than 40 mesh (greater than 420- μ m diameter) and another from powder of 200 mesh (74- μ m diameter) or finer. An excess gas pressure estimated at 0.5 atm would then be necessary inside the cathode to keep the coarsely porous layer filled with gas, while the finely porous layer is flooded. This estimate is necessarily rough, since porosities produced by sintering cannot be adequately predicted; an average porosity of 25% is expected.

In the original design, the porous cathode would be held in a cathode holder and cap of gold-palladium alloy by means of a bayonet fitting as sketched in Fig. 7. Inside the cathode holder the gas flow is guided by a baffle as shown in Fig. 8. The baffle is welded to an inner tube concentric with the outer tube. A mixture of H_2O and an inert carrier (see vertical cross section) flows toward the cathode holder through the annular space between the tubes, spreads radially and flows toward the cathode disk through slits in the circumference of the baffle which fits snugly in the holder. The gas velocity radially inward between the cathode disk and baffle increases by a factor of approximately 2. The increasing velocity gradient at the cathode plate causes an increased flux of gas into the plate, thereby compensating in part for the depletion in H_2O concentration due to the reaction upstream. The product gases diffusing away from the gas-liquid interface in the porous plate--*i.e.*, C_2H_2 , H_2 , possibly CO , and polymerization products of C_2H_2 --are swept into the gas stream exiting through the inner tube. The increase in radial velocity could be made greater by decreasing the angle, α , between the baffle and plate (Fig. 8), but this might cause an excessively uneven pressure distribution along the disk and the risk of entrainment of liquid with the exiting gas flow.

In view of the high cost and weight of materials (rhodium powder, in particular), and the structural problems associated with the use of gold, the possibility of an adequate substitute for gold-palladium alloy was explored. Low-carbon stainless steel--*e.g.*, Type 304L or 347--appear to have, in addition to anodic corrosion resistance (see above), a fair resistance to attack by lithium.

As a result of these considerations, the submerged part of the cathode holder has been made of stainless steel, Type 347. It is expected that the cathode can be maintained at a negative enough potential in and out of operation,

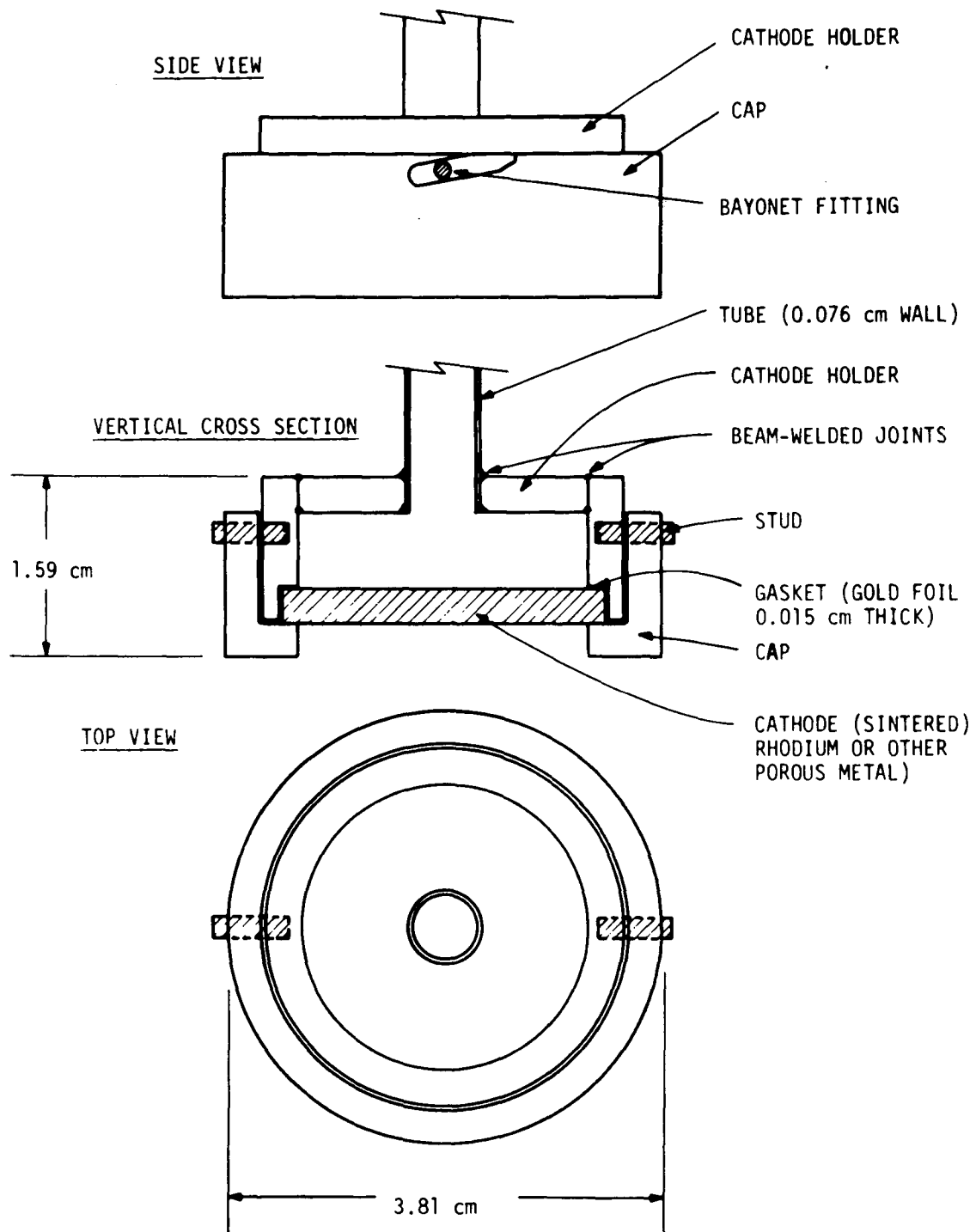


Fig. 7. Construction of Cathode Holder, Plate, and Cap

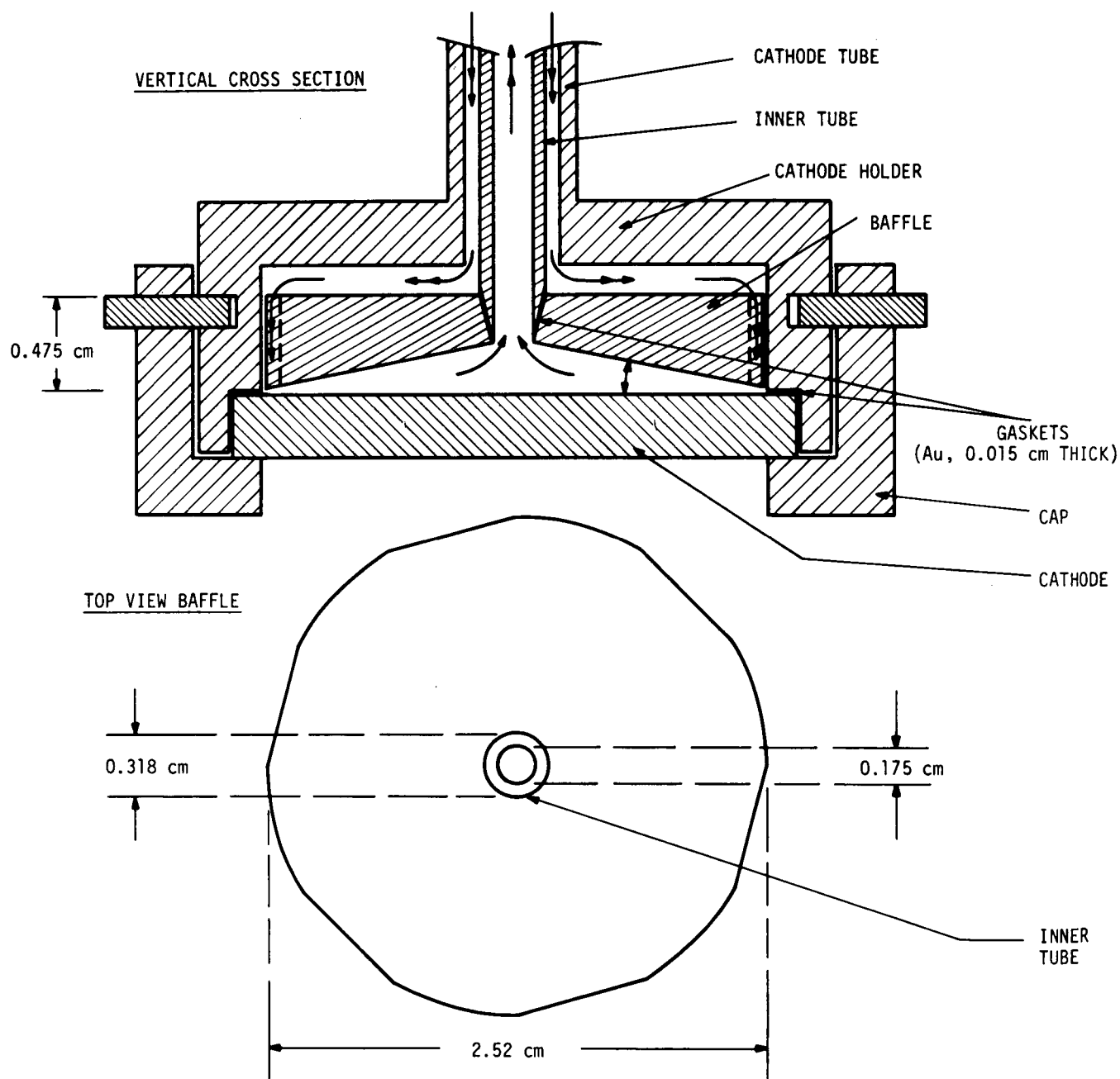


Fig. 8. Construction of Baffle Inside Cathode
(Dimensions in cm; Double-Headed Arrows
Indicate Flow Direction of the Gas)

to reduce the corrosion rate to an acceptably low level. Janz and Conte⁴ have found that niobium-stabilized steel is passivated in fused carbonates at a potential comparable to the corrosion potentials of gold-20 wt % palladium or platinum. The corrosion rate in a chloride-carbonate mixture, however, is likely to be greater than in carbonates only. Therefore, it is not ruled out that, eventually, a gold-palladium alloy cathode holder may have to be used, unless tests of various metals suitable as a cathode material would produce a better substitute.

Porous stainless steel and other metals were also considered for use in the cathode disk. Copper is an attractive possibility because it strongly inhibits carbon deposition in gas-phase reactions and, in molten salt, may enable acetylide formation to take place without carbon deposition. Nickel and cobalt in molten carbonates are, according to thermodynamic information,⁶ cathodically protected at the potential to be applied for acetylide formation. It is not certain, however, that these metals are also corrosion resistant in $\text{LiCl-Li}_2\text{CO}_3$ mixtures near the lithium-forming potential. For initial experiments single-porosity materials presently available (Table I) were selected.

From another point of view, a material with a large hydrogen overvoltage would be desirable since this would tend to suppress the parasitic hydrogen evolution reaction (see Introduction). No values are available for hydrogen overvoltages in molten salts. However, it can be reasonably assumed that the well-known correlation between the hydrogen overvoltage at a metal and the absorption enthalpy of hydrogen atoms at the same metal should also hold in ionic solvents. In that case, the order of decreasing hydrogen overvoltage will be similar to that in aqueous solvents (Table II).

To avoid complications due to corrosion reactions of dissimilar metals in contact, a Type 347 stainless steel porous cathode disk was selected for the initial experiments.

In the final design of the cathode holder, the inner tube leading to the baffle was split to make cathode assembly and disassembly more convenient. The two parts of the inner tube are now inserted from opposite ends of the outer cathode tube and joined by means of a screw fitting with an O-ring seal. Figure 1 of Appendix D shows the actual dimensions of the cathode as fabricated. Figure 9a is a photograph of the finished cathode with the inner tube partially exposed. Figure 9b shows the two parts of the inner tube separately.

The cathode holder as well as the anode assembly are capped by vacuum couplings to feed inner tubes through outer tubes such that their positions can be adjusted to some extent.

Gold-40 wt % palladium tubing for the anode was joined to the stainless steel parts by brazing with gold. Figure 2 of Appendix D shows the actual dimensions of the anode tubes. Figure 10a is a photograph of the lower end of the anode, with the inner tube partially exposed. Figure 10b shows the full anode assembled, with the inner tube partially exposed. In operation the inner tube is exposed only very slightly, if at all (see, *e.g.*, Fig. 6).

Table I
Materials Available for Porous Cathode Plates

		Ave. Pore Size, μm, nominal	Porosity, nominal	M.P., °C	
Nb	foam ^a	12	?	2500	
	mesh	700			
Mo	foam	25	0.78	2600	
	foam	75	0.83		
	mesh	1280			
Cu	felt	43	0.80	1083	
	powder	300-400, 100			
Fe	mesh ^a	400		1540	
	powder	400, 44			
Stainless Steel 302	felt	27	0.90	1420	
	felt	65	0.92		
	felt	30	0.80		
Stainless Steel 347	mesh	27	0.90	1430	
	mesh	400, 700			
Stainless Steel 430	sponge	100-200	0.90	1510	
	Ni	felt	85	0.86	1455
		60	0.80		
		powder	1		
Co	powder	100, 1		1495	
Cr	foam ^b	25	0.70-0.80	1800	

^aAppreciably oxidized.

^bDual porosity.

Table II
Metals in Order of Decreasing Hydrogen
Overvoltage in Aqueous Solution^a

Order of magnitude of exchange current density	
Pb] 10 ⁻¹² A/cm ²
Hg	
Tl	
Nb] 10 ⁻⁹ to 10 ⁻⁶ A/cm ²
Cd	
(Ta)	
Al	
(Be)	
Mo	
Ga	
Au	
Cu	
Fe	
(Cr)	
(Co)] 10 ⁻⁴ A/cm ²
(Mn)	
Ag	
(W)	
Ni	
Pt] 10 ⁻⁴ A/cm ²
Rh	
Pd	

aValues from Ref. 15, Fig. 1. Exchange-current densities are accurate to an order of magnitude only. Metals between parentheses inserted on the basis of other information in Ref. 15.

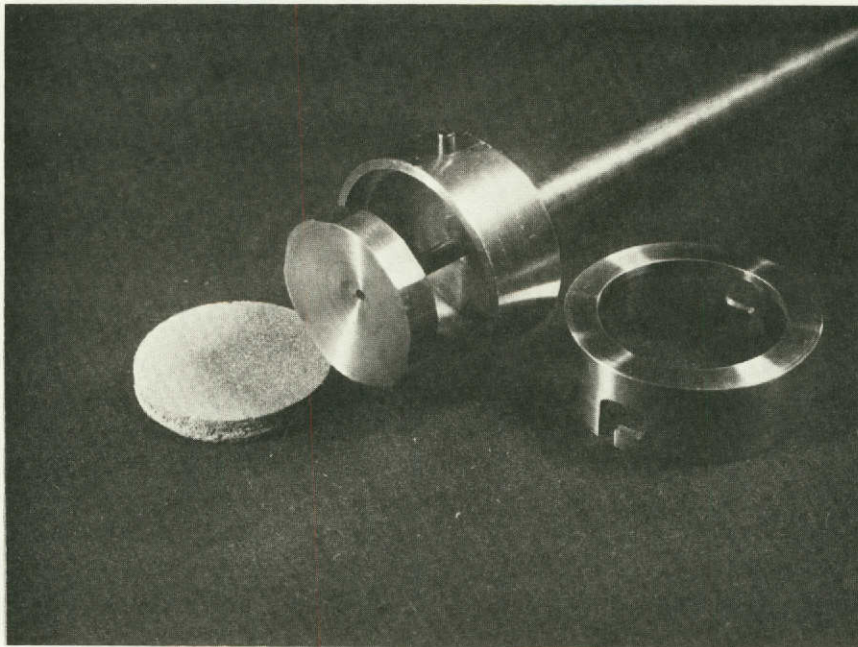


Fig. 9a. Cathode With Inner Tube Partially Exposed

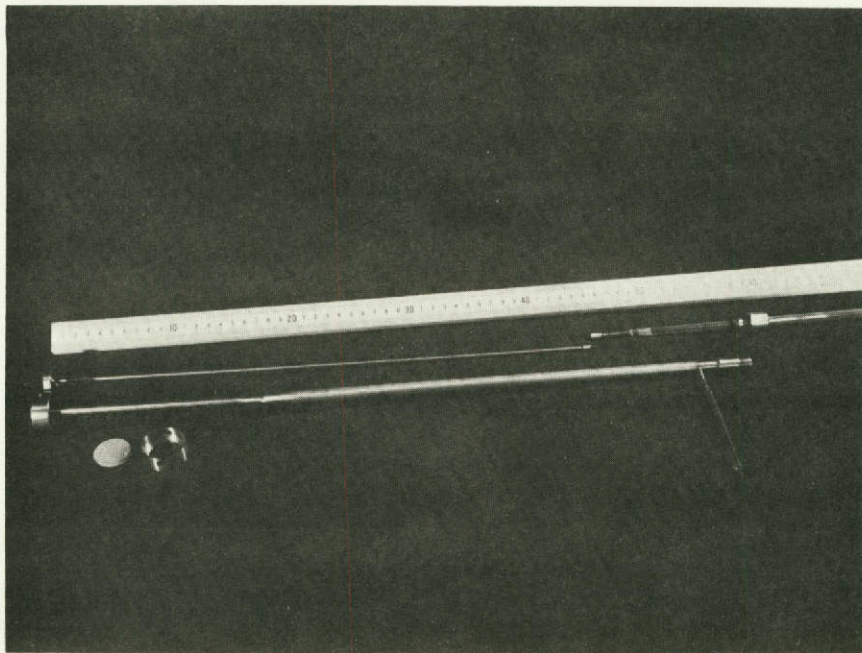


Fig. 9b. Inner and Outer Tubes of the Cathode, Disassembled



Fig. 10a. Lower End of the Anode Assembly
(Inner Tube Partially Exposed)

Reproduced from
best available copy. 

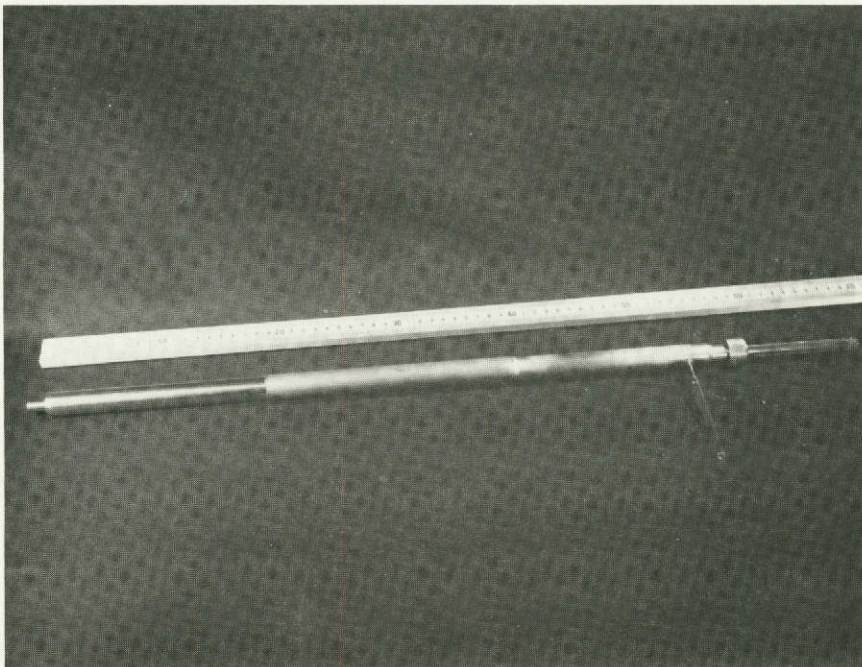


Fig. 10b. Full Anode Assembly (Inner
Tube Partially Exposed)

2. Electrolyte

For the initial experiments, it was decided to use the LiCl-KCl eutectic (m.p. 352°C; operating temperature 400-450°C) on the basis of positive results (C₂H₂ detection tests) reported in the United Aircraft work.⁸ However, LiCl-RbCl eutectic (m.p. 318°C; operating temperature 375°C and higher) was also kept available.

In addition, the LiCl-CaCl₂ eutectic (m.p. 496°C; operating temperature approximately 575°C) was considered. Calcium carbide has a fairly high stability (see Appendix A); this may offset the disadvantage of having to operate at a higher temperature. Lithium chloride-BaCl₂ mixtures (m.p. less than 600°C with more than 20 wt % BaCl₂) are of potential interest since BaCl₂ is presumably fairly stable.

B. Gas Supply System and Furnace

1. Glovebox Atmosphere

The experiments were carried out in a glovebox so that different atmospheres could be maintained over the electrolytic cell. For reasons of safety the originally planned 67 vol % CO₂-33 vol % O₂ atmosphere, which would have made the gold container lining a fairly stable reference electrode, had to be abandoned. Instead, nitrogen was used in the glovebox and argon was used to blanket the electrolyte. In later experiments CO₂ was mixed with the argon to stabilize the potentials of unpolarized conductors (thermocouple sheath, sparger, outer tube of anode, beaker lining). As part of the safety precautions, a nitrogen purging stream of approximately 2 liter/min had to be maintained. The cell itself, located in a furnace well attached to the glovebox, was continually sparged, or blanketed, by approximately 400 ml/min argon and/or CO₂. In the design of a practical cell, the possible formation of explosive gas mixtures must be avoided by preventing the escape of gases from the anode and cathode through proper control of the liquid-gas interface in each of the electrodes.

2. Furnace

The cell is contained in a 12.7-cm (5-inch) diameter furnace well which is attached to the glovebox and surrounded by a heating mantle. The furnace well is provided with heat-insulating baffles (see Fig. 5) and the electrolyte container is seated in a mantle of high thermal conductivity (copper, aluminum), so that the temperature gradient toward the bottom of the well is negative. It can be controlled by means of a separate heating plate attached to the bottom of the well.

3. Gas-Supply System

A simplified flow diagram for the gas-supply system is presented in Fig. 11. To facilitate gas-chromatographic analysis of the product gases, different carrier gases were used for the cathode and anode gas flow: helium for the anode stream, argon for the cathode stream. Water was injected into the cathode feed stream by a precision syringe drive.

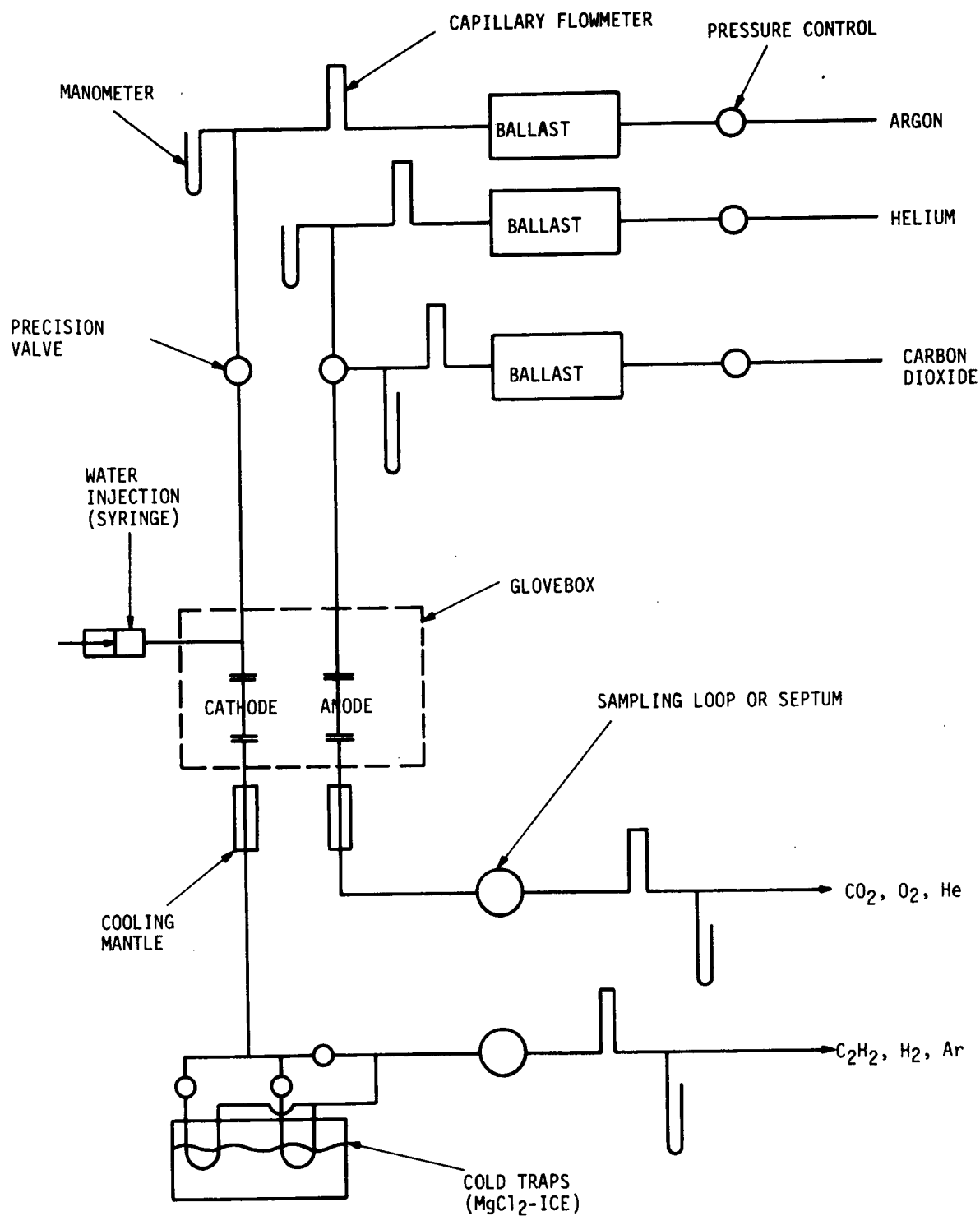


Fig. 11. Schematic Flow Diagram of Gas-Supply System

Low flow rates are to be expected if operation of the cell is successful: *e.g.*, 100 mA/cm² at 5 cm² of cathode would correspond to 0.67 ml/min(STP) gas conversion at the cathode, according to reaction (1). Therefore, gas flow rates were measured by capillary flowmeters and the volume of the gas-supply system was minimized by using 3.2-mm (1/8-in.) diameter tubing (glass or copper) wherever possible (see Table B.1 of Appendix B).

The design of the capillary flowmeters to be used at five points in the gas train is shown in Fig. 12. Each flowmeter has an interchangeable capillary of 10-cm length. Three different bores were used. The flowmeter has two 12.5-cm U-tubes, one using silicone oil as a manometer liquid, the other mercury. The full-scale flow range covered by the three capillaries and two manometer liquids is 0.2 to 132 ml/min (0.015 cp viscosity, 25°C). The dead volume of the manometer is minimized by using 0.2-cm I.D. tubing and Rotaflo* stopcocks with a 1-mm capillary bore. The complete gas supply system is shown in Appendix B. Glass-to-metal connections are Pyrex-to-Kovar graded seals. Metal-to-metal connections are either silver-soldered (approximately 300 joints) or consist of Swagelock fittings (approximately 75). Most connections were individually checked for leaks before they were inserted into the system. This time-consuming inspection was necessary since the expected gas pressures will be 1.5 atm in the cathode line and somewhat less in the anode line, and flow rates will be low, between 1 and 100 ml/min. Downstream of the exit capillary flowmeters, thick-walled rubber tubing has been used, which ends in an open intake of the room exhaust system.

C. Gas Analysis

Representative samples of the anode and cathode product gases have been made up and analyzed completely by gas chromatography. The objective was to check if a satisfactory material balance (preferably to approximately 1 vol %) could be obtained using routinely available equipment and standardizing by the pure component gases only.

Another objective was to check the accuracy with which component fractions can be measured in this manner.

The results (reported in Appendix C) indicated that a 3-5% accuracy can be expected in the analysis of component gas fractions by existing equipment. The reproducibility of the analyses is better than 1%, provided that a sampling loop is used instead of the septum-and-syringe technique. To obtain a better than 1 vol % material balance, calibration of the chromatographic equipment would have to be more elaborate and exact than can be warranted at present.

In view of the uncertainty about the composition of initial gas samples, it was decided that mass spectrometry would be used to identify components of these samples. In general, any gas present in more than 0.5% concentration can be detected and analyzed quantitatively.

*Registered trademark of Quickfit Corp., Fairfield, N. J.

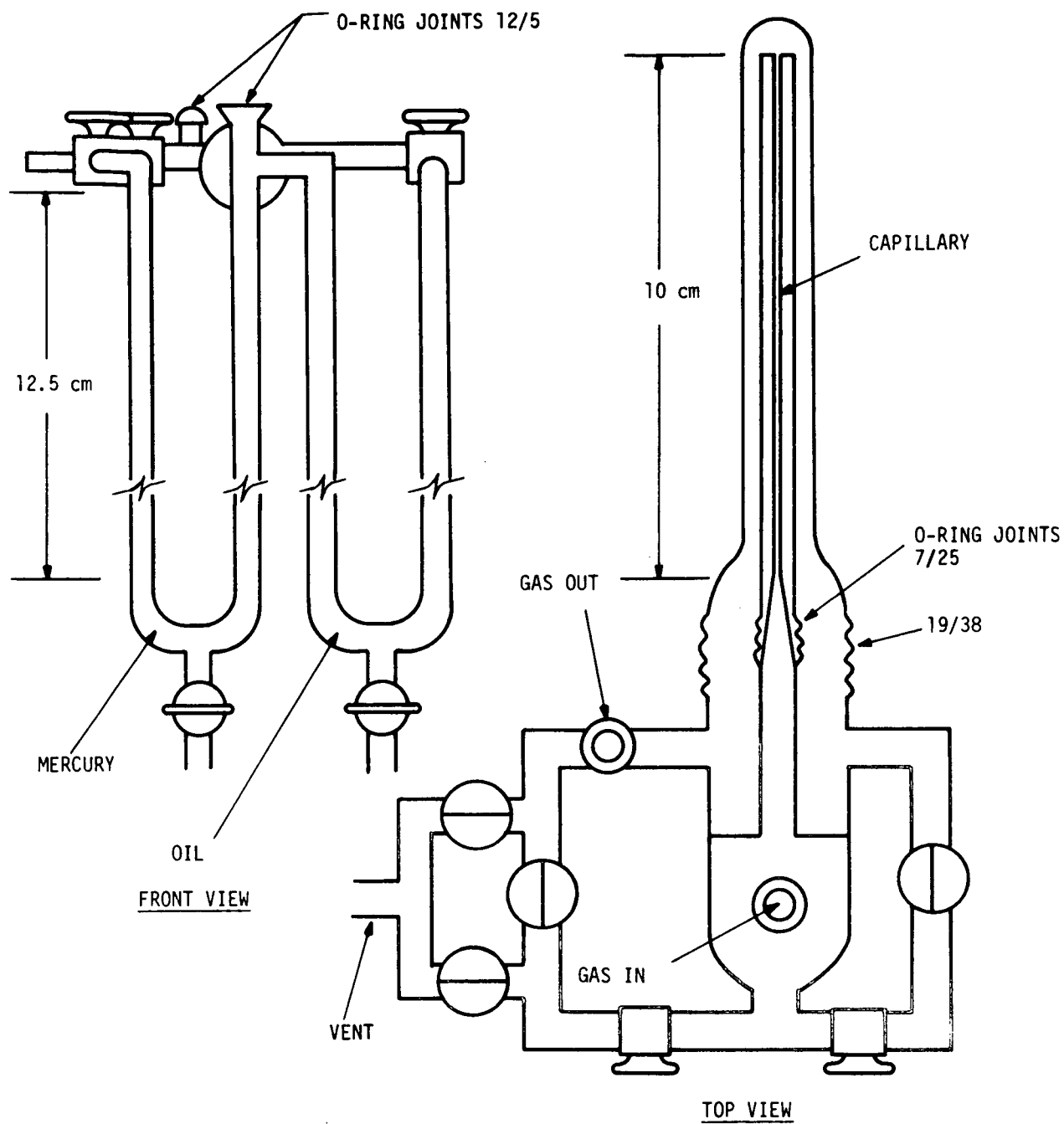


Fig. 12. Design of Capillary Flowmeter (Schematic); Capillary Bore: 0.010 cm (0.004 in), 0.015 cm (0.006 in), or 0.028 cm (0.011 in)

D. Experimental Approach

For a given electrolyte composition and cathode material, the cell operation may depend on

1. applied potential;
2. water concentration in the cathode feed gas;
3. cathode-gas flow rate;
4. CO₂ concentration in the anode feed gas;
5. anode-gas flow rate;
6. temperature.

Gas pressure, especially at the cathode side, may also be important but is relatively fixed by the need to localize the gas-liquid interface in the porous cathode; *i.e.*, it depends on cathode structure, electrolyte composition and temperature. Current density is considered to be a function of applied cell potential, gas compositions, and flow rates.

The variables listed above are arranged in the order of expected importance for a test of the C₂H₂-producing capability of a given cell. Of all the possible systematic variations, the following sequence was chosen for use in the experimental work.

1. Stepped-Potential Scanning

The gas flow rates and compositions are fixed. The anode-gas flow is set at, *e.g.*, 10 ml/min (STP) 75% CO₂. This is more than sufficient to provide all the CO₂ to be converted to either C₂H₂ or carbon or CO, at a rate corresponding to 0.6 A total current, *i.e.*, the current supply capacity. The cathode-gas flow is set at 20 ml/min (STP) 40% H₂O. This is more than sufficient to feed a 0.6 A current, whether conversion is to H₂, C₂H₂, C₂H₄ or CH₄. The applied potential is increased from approximately 1.25 V to beyond 1.75 V in steps of, *e.g.*, 0.1 V. The qualitative test for C₂H₂ can be used at each step or the gas can be sampled and analyzed. At a semiquantitative level, without analysis, insight can be gained by accurate measurement of the increase or decrease of the cathode and anode gas flows and of the total current level, provided these are all steady during a typical sampling time. This amounts to an estimate of the electrochemical equivalence of the cathodic process.

For purposes of comparison with experimental potentials, the theoretical standard cell potentials have been calculated for a number of possible cathode reactions in a melt containing Li⁺, CO₃⁼ and OH⁻ ions as well as dissolved nitrogen. The overall cell reactions, as well as the cell potentials at several temperatures, are shown in Table III. The values are based on free energies of formation given in standard tables.⁹

Table III
Cell Potentials for Reactions (9)-(15)

Reaction	EMF, volts				
	Temp., °K				
	298	600	700	800	900
$\text{Li}_2\text{O} \xrightarrow{2e^-} 2 \text{Li} + 1/2 \text{O}_2$ (9)	2.91	2.71	2.63	2.56	2.49
$3/2 \text{Li}_2\text{O} + 1/2 \text{N}_2 \xrightarrow{3e^-} \text{Li}_3\text{N} + 3/4 \text{O}_2$ (10)	2.38	2.34	2.33	2.31	2.30
$\text{Li}_2\text{CO}_3 \xrightarrow{2e^-} \text{Li}_2\text{O} + \text{CO} + 1/2 \text{O}_2$ (11)	2.25	1.86	1.74	1.62	1.50
$\text{LiOH} \xrightarrow{2e^-} \text{LiH} + 1/2 \text{O}_2$ (12)	1.92	1.80	1.77	1.73	1.71
$\text{Li}_2\text{CO}_3 \xrightarrow{5e^-} 1/2 \text{Li}_2\text{C}_2 + 1/2 \text{Li}_2\text{O} + 5/4 \text{O}_2$ (13)	1.71	1.57	1.53	1.49	1.45
$\text{Li}_2\text{CO}_3 \xrightarrow{4e^-} \text{C} + \text{Li}_2\text{O} + \text{O}_2$ (14)	1.48	1.36	1.32	1.28	1.25
$2 \text{LiOH} \xrightarrow{2e^-} \text{H}_2 + \text{Li}_2\text{O} + 1/2 \text{O}_2$ (15)	1.64	1.35	1.26	1.19	1.11

Assuming cell reactions (11), (13), (14), and (15) to occur exclusively, stoichiometric calculations have been made. These relate the increase in cathode and anode gas-flow rates per coulomb passed directly to (1) the fraction of CO_2 converted to CO , (2) the number of H_2O molecules converted per mole of CO_2 reacted. These relationships will be used in the interpretation of experimental results.

2. Optimization of Gas Composition

Once a potential range has been found in which C_2H_2 is produced, the cell is best operated at a particular applied potential in this range and the gas compositions are varied at fixed total flow rates. The cathode H_2O feed rate is diminished first while the anode-gas flow rate is unchanged. The objective is to find the $\text{H}_2\text{O}/\text{CO}_2$ flow ratio at which C_2H_2 production is replaced by carbon production. In principle, qualitative testing for C_2H_2 would suffice for this purpose. A complete material balance would be desirable for a $\text{H}_2\text{O}/\text{CO}_2$ ratio just above the minimum for C_2H_2 formation, if such a minimum exists.

The procedure is repeated for several decreasing levels of CO_2 content of the anode gas at the same flow rate as before. Correlation of the C_2H_2 production at minimal $\text{H}_2\text{O}/\text{CO}_2$ ratio with the current yields information on possible transport limitations of the cell with respect to CO_2 .

3. Effect of Total Gas Flow Rates

If both a potential range and a minimal $\text{H}_2\text{O}/\text{CO}_2$ flow ratio for C_2H_2 formation can be established, the effect of varying the total gas flow rates may be studied. Especially at the cathode side, a transport limitation may exist because of product-gas diffusion from the gas-liquid interface to the main gas stream.

4. Constant-Current Operation

For a particularly favorable and steady combination of applied potential, gas compositions and gas flow rates, constant-current operation during several hours would be the most reliable method to ascertain the reactions involved in the cell since it would allow an accurate measurement of the amount of H_2O consumed.

E. Initial Experiments

The initial experiments were aimed primarily at qualitative detection of C_2H_2 formation by precipitation of Cu_2C_2 (red) in ammoniacal cuprous solution. Another objective of the initial experiments was to obtain a polarization curve which would yield indications of the potential range in which C_2H_2 formation would occur.

The electrolyte was LiCl-KCl eutectic with additions of Li_2O (2 wt % or 1.1 mol %), Li_2CO_3 (0.2 wt %), and LiOH (0.1 wt %), separately vacuum dried. The cell temperature was approximately 430°C .

The cathode was a Feltmetal* disk of Type 347 stainless steel, diameter 2.86 cm, 0.30 cm thick, porosity 0.79, average pore size 27 μm . The disk was pressed against a sealing ring of gold, 0.17 mm thick, by a bayonet fitting. The cathode housing and the cap of the fitting were of Type 347 stainless steel. The exposed area of the cathode was 3.9 cm^2 . The gas inside the cathode holder flowed radially inward over the cathode disk, through a slit of 0.1-cm thickness, at a speed of approximately 1 cm/sec.

The anode lead was a gold wire of 0.38 mm dia which formed a screen of 2.4- cm^2 area inside the open end of the gold-palladium inner tube of the anode. The lead was fed out through a vacuum coupling. The outer tube (shield) of the anode was prevented from touching the inner tube by an alumina sleeve above the electrolyte level.

Initial experiments had to be discontinued temporarily because the cathode gas exit tube cracked during adjustment of its depth of immersion in the electrolyte.

The thermocouple sheath, of Type 347 stainless steel, had a consistently negative open-circuit potential with respect to the grounded gold beaker. The potential differences, initially -56 mV, reached a value of -300 mV after 5 hr and then leveled off at approximately -100 mV. The sparger tube, also of Type 347 stainless steel, behaved similarly. During sparging of argon, the open-circuit potentials of the various stainless steel parts became markedly more negative (thermocouple -400 mV, sparger and cathode -200 mV) and unstable. The open-circuit potential of the gold-palladium anode was 200 to 300 mV more negative than the gold beaker. It did not vary much with time.

After the cell had been disassembled, inspection of the stainless steel parts showed corrosion (intergranular corrosion and pitting) of an area 1 to 5 cm above the electrolyte level. Apparently the electrolyte crept up to the stainless steel, forming a thin layer, which, together with the hot gas atmosphere, caused severe corrosion by breakdown and flaking of the oxide layer. The stainless steel surface below the electrolyte level was covered and apparently protected by a fairly coherent black layer which could not easily be removed mechanically or chemically. The gold beaker and gold-palladium tubes showed no signs of attack. The same type of corrosion was observed in the second run.

The second run was made with new electrolyte of the same composition (97.7 wt % LiCl-KCl eutectic, 2 wt % Li_2O , 0.2 wt % Li_2CO_3 , 0.1 wt % LiOH) at 426°C. A new cathode disk of Type 347 stainless steel Feltmetal (exposed area, 3.87 cm^2 ; porosity, 0.79; average pore size, 27 μm) was installed. Constant input gas flows were established as indicated in Fig. 13. An attempt was made to obtain a reasonable gas balance. The polarization curve shown in Fig. 13 was obtained by applying a stepwise increasing cell potential. The steps were 100 mV each, applied to the cell and a 1-ohm current-measuring resistance in series with the cell. Each step lasted 5 min, followed by 3 min open circuit. The current usually reached a steady value after 1 to 3 min, except

*Registered trade mark, Brunswick Corp.

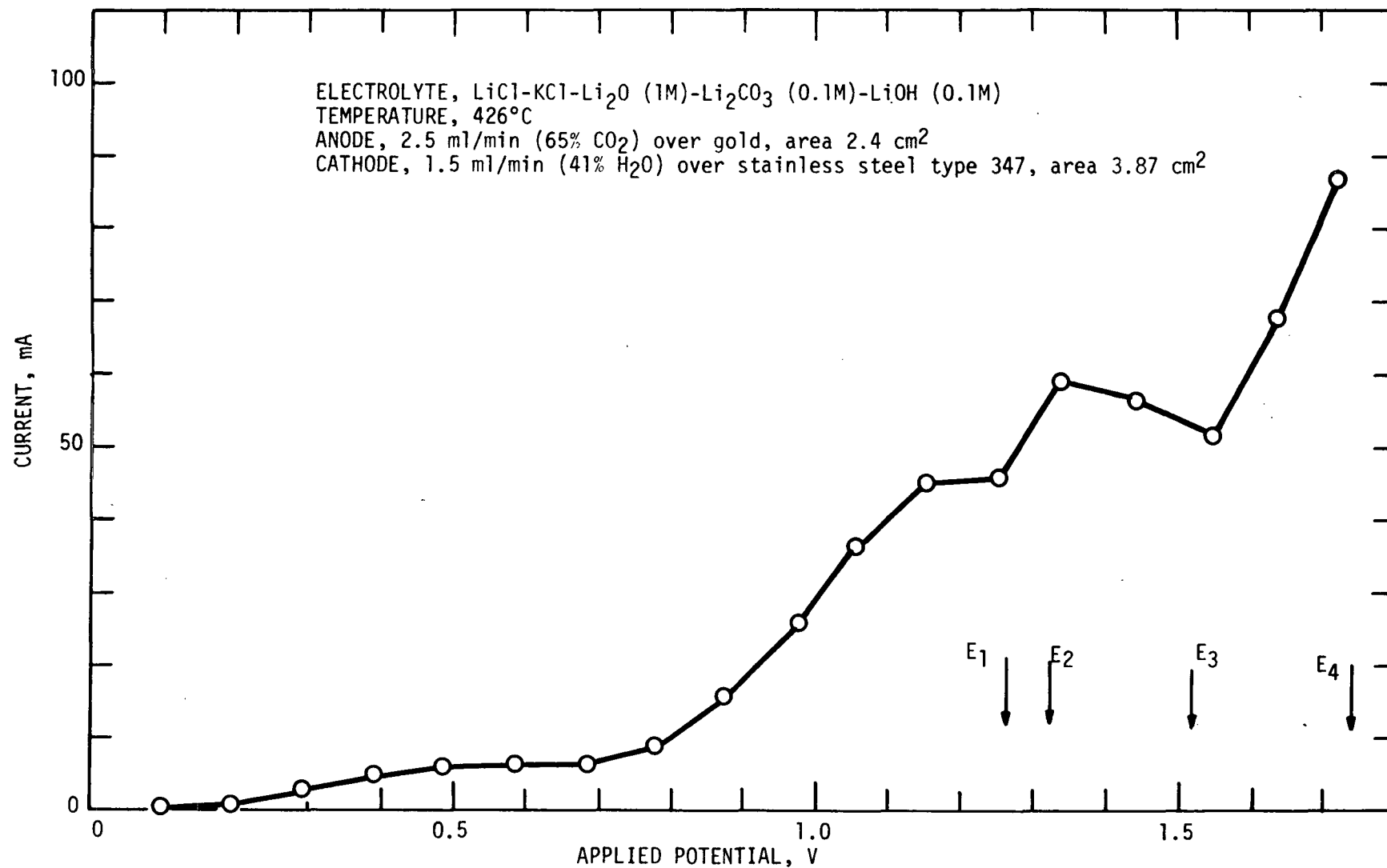


Fig. 13. Polarization Curve

in the voltage range between 1.3 and 1.6 V, where it kept decreasing. At 1500 mV applied potential, a value of 52 mA was measured after 5 min, decreasing to 32 mA after approximately 10 min.

Figure 13 indicates a plateau between 1.1 and 1.3 V, probably due to hydrogen formation (theoretical cell potential at 700°K shown as E_1), and a higher but indistinct plateau between 1.3 and 1.6 V. The latter plateau is very likely related to carbonate reduction, but it cannot be concluded at this point whether carbon deposition (theoretical potential E_2) or C_2H_2 formation (theoretical potential E_3) is prevalent. The increase in current above 1.6 V is unexpected; the decomposition potential of Li_2O at 700°K is 2.63 V. It may be caused by CO formation from carbonate (theoretical potential E_4). Plans are being made to insert a reference electrode to provide a more definite interpretation of the cathode reaction. This will also permit a better understanding of corrosion reactions and their effect upon cathode behavior.

To establish the gas flows through the anode and cathode without sparging into the electrolyte, a slight vacuum was applied to the downstream side. Even so, a mass balance at open circuit could not be established satisfactorily, probably because of remaining leaks near the exit of the line. This also prevented the qualitative test for C_2H_2 .

Samples of cathode and anode product gas were taken during a 15-min run at 1500 mV applied potential. Analysis of the samples by mass spectrometry showed that most of the entering cathode gas and all of the anode gas had probably been sparged into the electrolyte because of leaks in the downstream, low-pressure part of the cathode and anode gas lines.

III. CONCLUSIONS AND STATUS

Initial experiments with a porous stainless steel cathode in a LiCl-KCl electrolyte with small additions of oxide, carbonate and hydroxide show a current plateau between 1.1 and 1.3 V, probably due to hydrogen formation, and a plateau between 1.3 and 1.6 V which is tentatively assigned to the reduction of carbonate ions. In this potential range the current continues to decrease and reaches a fairly steady value only after 10 or more minutes.

Stainless steel parts in contact with the electrolyte show severe corrosion (grain boundary attack and pitting) just above the electrolyte level after 100 hr at open circuit.

Present efforts are directed toward identification of the cathode products at the 1.3-1.6 V current plateau. Difficulties encountered in obtaining a gas balance make it necessary to give special attention to maintaining leak-free gas trains at very low flow rates (1-10 ml/min).

The corrosion of stainless steel at open circuit in the electrolyte indicates the need for investigation of the corrosion behavior of various metals in the electrolytes used. A reference electrode for this purpose is being designed.

APPENDIX A
THERMODYNAMIC DATA ON ACETYLIDES

Table A.I

Standard Enthalpy and Gibbs Energy of Formation of
Alkaline and Alkaline Earth Acetylides (in kcal/mol)

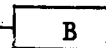
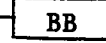
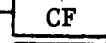
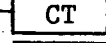


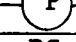
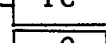
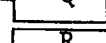
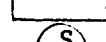

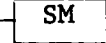
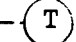
		ΔH_f°			ΔG_f°			
T(°K)→		298.15	700	1000	298.15	700	1000	1300
Ref:								
Li ₂ C ₂	9	-14.20	-14.96	-14.39	-13.41	-11.92	-10.71	-9.70
	10				-11.2	-5.7	-1.4	+2.9
Na ₂ C ₂	11	+4.80	+6.31	+8.63	+5.02	+5.35	+4.62	
	12	+4.1			+8.5			
MgC ₂	9	+21.00	+22.10	+20.14	+20.27	+18.65	+17.31	+16.47
	12				+21.0			
CaC ₂	13	-15.5	-13.9	-12.5	-16.2	-18.6	-21.2	
	14	-14.3			-15.5			
	12	-14.1			-15.4			
SrC ₂	14	-18.0						
	12	-20.2						
BaC ₂	14	-18.0						
	12	-19.5			-15.2 ^a			

^aCalculated from ΔH_f° and S° at 298.15°K given by Ref. 12.

APPENDIX B
GAS SUPPLY SYSTEM

Legend and Symbols for Figure B.1.





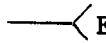
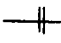

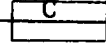


Legend:

	Ballast
	Bubbler
	Capillary Flowmeter
	Cold Trap (MgCl ₂ -Ice)
	Filter
	Manometer (Mercury U-Tube)
	Pressure Gage
	Pressure Control
	Qualitative Test for C ₂ H ₂
	Rotameter
	Septum
SL	Sampling Loop
	Soap Membrane Flow Meter
	Temperature Indicator

Heavy Line: Main Anode and Cathode Flow

Dashed Windows: Glass Parts

Symbols:

	Metering Valve
	Toggle Valve
	Precision Metering Valve
	Four-way Port
	Open-ended Tube (to Exhaust)
	O-ring Glass Joint
	Heating Mantle
	Cooling Mantle
	Heating Lamp
	Fan

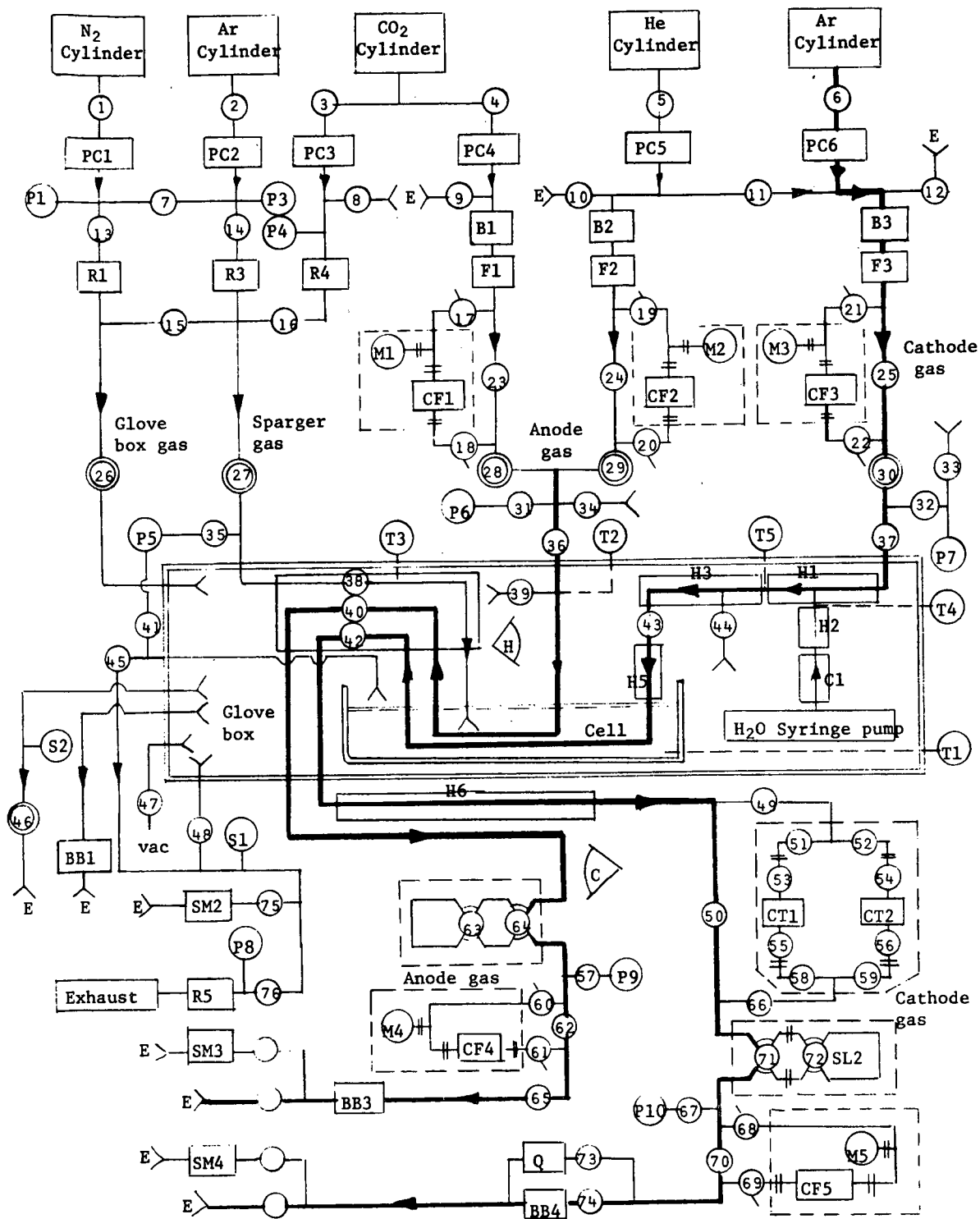


Fig. B.1. Schematic Flow Diagram of the Gas Supply System

Table B.I
Estimated Hold-up Volumes

	Volume, ml	
	Cathode	Anode
No by-passing		
Cylinder to exhaust	700	580
Flowmeter to flowmeter	210	270
Cell to cold trap	20	-
Cell to sampling loop	60	90
Cell to exhaust	350	390
Flowmeters, sampling loops, and cold trap by-passed		
Cylinder to exhaust	390	580
Cylinder to by-pass flowmeter (CF3)	200	(CF1,2) 170
Flowmeter to flowmeter	40	120
Cell to exhaust	175	240
Capillary flowmeter	130 ml each	
Cold trap	30 ml each	
Sampling loop	15 ml each	
Bubbler	100 ml each	
Furnace well	4 l	
Glovebox	750 l	

APPENDIX C
GAS ANALYSIS OF SYNTHETIC SAMPLES

Anode Gas

The anode gas sample consisted of approximately equal volumes of CO_2 , O_2 , and He, at a total pressure of approximately 1.5 atm. Carbon dioxide was analyzed on a silica-gel column, using a helium carrier and a thermal conductivity detector. Oxygen and helium were analyzed on a molecular sieve column, using an argon carrier and a thermal conductivity detector. Initially, 50- μl samples were taken through a septum, but air leakage made the oxygen peak irreproducible. The results of sampling with a 5-ml loop at low pressures are shown in Table C.I. Calibration by the pure component gases at the pressure of the sample yielded a 99.6% material balance. Individual component measurements were reproducible within 2-3%. The CO_2 values were somewhat on the high side, and the O_2 values on the low side, but within 3% of the true value, so a 1% accuracy for the total material balance is indicated.

This result was considered encouraging, especially since oxygen was analyzed using argon as the carrier gas. In the actual analysis a 1-ml sampling loop is used, and samples are taken at 1 to 1.5 atm total pressure.

Cathode Gas

The cathode gas consisted of approximately equal volumes of C_2H_2 , H_2 , and Ar, at a total pressure of approximately 1.5 atm. Acetylene was analyzed on a Porapak* column, using a helium-hydrogen carrier and a flame ionization detector. Hydrogen was analyzed on a molecular sieve column, using an argon carrier and a thermal conductivity detector. Argon was analyzed on a silica gel column using helium as a carrier and a thermal conductivity detector. One-ml samples were taken at 1000-mm pressure through a septum. With this sampling pressure and volume, air leaks appeared to be unimportant. However, the accuracy of the component-fraction determination (see Table C.II) was less satisfactory than in the case of the anodic sample. The hydrogen and argon analyses were about 6% higher than the make-up values, and the C_2H_2 analysis was about 8% lower. Reproducibility of the component fractions was $\pm 3\%$ as in the case of the anode gas. The material balance, therefore, was less satisfactory than it appeared to be (101.8%) due to compensating errors.

In subsequent checks of the detector calibration, it was found that C_2H_2 calibration was reproducible only to $\pm 6\%$ when performed at 333 mm Hg. To eliminate the septum and syringe as a source of variability, a 1-ml loop was used in subsequent samplings.

*Registered Trademark of Waters Associates, Inc., Framingham, Mass.

Table C.I
Analysis of Anode Gas Sample

Gas	Make-up		Calibration		Sample Analysis		
	Pressure	Vol. %	Pressure, Torr	Response, GCU/ μ mol) ^a	Pressure, Torr	Volume, ml	Vol. %
CO ₂	408	34.1	77.5	3053 ^b	207	5.98	34.8
O ₂	401	33.5	49.5	193 ^c	25.5	5.69	33.4
			198	200 ^c	129.0	5.69	31.5
						ave:	32.5
He	387	32.4	9.5	1146 ^b	25.5	5.69	31.9
			45	1048 ^b	129.0	5.69	32.7
						ave:	32.2
Total	1196.0	100.0				ave:	99.6

^aBased on peak height.

^bWith pure gas.

^cWith air.

Table C.II
Analysis of Cathode Gas Sample, Using Syringe Sampling

Gas	Make-up		Calibration ^a		Sample Analysis		
	Pressure, Torr	Vol. %	Pressure, Torr	Response, GCU/ μ mol)	Pressure, Torr	Volume, ml	Vol. %
C ₂ H ₂	435.0	33.9	341	2352	978.0	0.50	31.6
					966.7	0.50	31.1
					953.6	0.50	32.0
						ave:	31.6
H ₂	442.5	33.1	333	1317	988.0	1.00	34.9
					966.0	1.00	35.5
						ave:	35.2
Ar	440.5	33.0	331.5	1412	983.0	1.00	34.1
					960.3	1.00	35.8
					975.6	1.00	35.0
Total	1336.0	100.0				ave:	35.0
						ave:	101.8

^aWith pure gas.

The results are given in Table C.III. Measurement of the peak heights was considered to be sufficiently accurate for the present purpose. From these results one concludes that

- (1) the reproducibility of the measurements is quite satisfactory (within 1%) and
- (2) the accuracy of the C_2H_2 and hydrogen measurements is somewhat less satisfactory. The deviations from the make-up composition are now positive for all three components, especially for the C_2H_2 and hydrogen. This result indicates that the response of the columns and/or detector to the pure component gases at one third of the sample pressure is 3-5% low in the case of C_2H_2 and hydrogen.

To check if non-ideality of the gas sample might be responsible for apparent deviations, compressibilities of the component gases at 1-2 atm pressure were calculated from the second virial coefficient as estimated by the method of Pitzer and Curl.¹⁶ Table C.IV shows that the corrections for non-ideality are far smaller than the deviations encountered in the gas-chromatographic analyses. From the data of Table C.IV the actual mole percentages in the sample mixture of Table C.III were found to be

C_2H_2 32.55% (*i.e.*, 0.07% higher than the ideal value).

H_2 33.57% (0.09% lower), Ar 33.88% (0.02% higher).

Table C.V compares responses in gas chromatographic units (GCU) per μ mole for the pure components and the mixed-gas samples. In all cases the sample was approximately 20 μ mole. The total sample pressure appears to have an influence on the peak-height response.

These analyses indicate that a 3-5% accuracy can be expected in the analysis of component gas fractions by existing equipment, if the detector is calibrated by the pure component gas at a pressure corresponding to the partial pressure in the mixture. To obtain greater accuracy, a set of standard calibration mixtures would have to be used. The values of Table C.IV show that such mixtures can be made up volumetrically with less than 1% error. The reproducibility of gas-chromatographic analysis is better than 1%, provided that a sampling loop is used instead of the septum-and-syringe technique.

Table C. III
Analysis of Second Cathode Gas Sample, Using 1-ml Loop^a

Gas	Make-up		Calibration		Sample Analysis	
	Pressure, Torr	Vol. %	Pressure, Torr	Response, GCU/ μ mol	Pressure, Torr	Vol. %
C ₂ H ₂	485.0	32.5	346	1935	982	33.5
			341	1999	987	33.1
				ave: 1967	994	33.8
						ave: 33.5
H ₂	502.5	33.6	335	1576	984	35.3
			336	1579	995	34.9
			324	1593	953.5	35.2
				ave: 1583	945	35.5
Ar	505.5	33.9				ave: 35.2
			343	905	986	34.0
			346	892	986.5	34.2
				ave: 899	985.5	34.1
Total	1493.0	100.0				ave: 34.1
						ave: 102.8

^aCalibration and analysis samples were always 1.116 ml in volume.

Table C. IV
Second Virial Coefficients and Compressibility
Factors of Reactant and Product Component Gases

	B, cm ³ /mol	Z (at 1 atm)	Z (at 1.5 atm)	Z (at 2 atm)
CO ₂	-126.4	0.995	0.992	0.990
O ₂	-15.7	0.999	0.999	0.999
He	+17.1	1.001	1.001	1.001
C ₂ H ₂	-155.5	0.994	0.990	0.987
H ₂	+16.5	1.001	1.001	1.001
Ar	-15.5	0.999	0.999	0.999

B = second virial coefficient.

Z = compressibility factor.

Table C.V
Peak-Height Response for Pure Components
and for Mixed Gas Samples

Gas	Carrier	Pressure, Torr	Vol. %	Quantity, μ mol	Response Ave. \pm St. Dev., GCU/ μ mol	Number of Trials
C ₂ H ₂	H ₂ + He	340	100	20.7	1970 \pm 40	3
		988	32.5	19.2	2020 \pm 20	3
H ₂	Ar	332	100	19.9	1580 \pm 20	3
		967	33.7	19.5	1660 \pm 10	4
Ar	He	345	100	20.6	900 \pm 10	1
		986	33.8	20.0	906 \pm 1	3

APPENDIX D
DIMENSIONAL DRAWINGS OF ELECTRODES

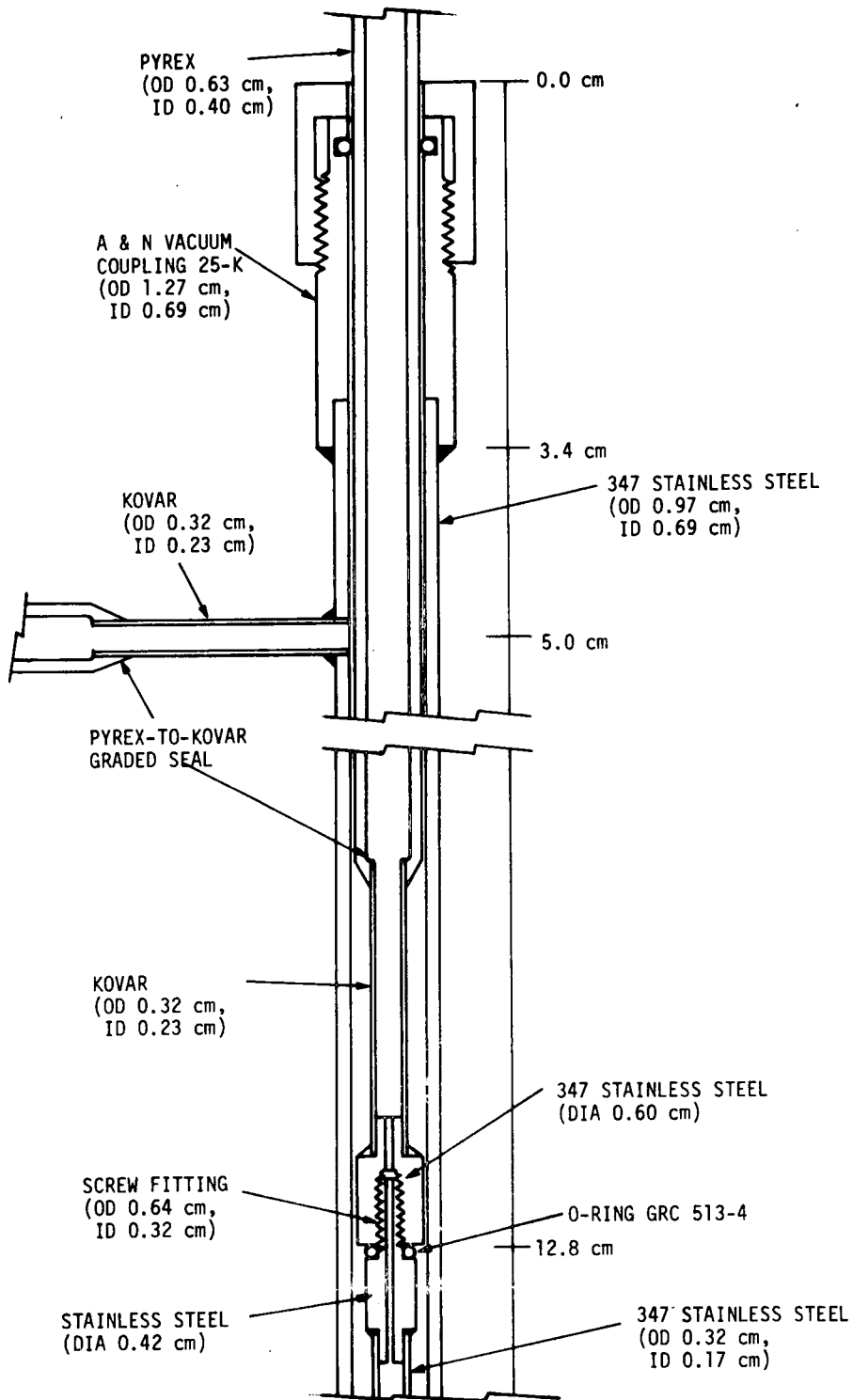


Fig. D.1a. Cathode, Upper Part (Vertical Section)

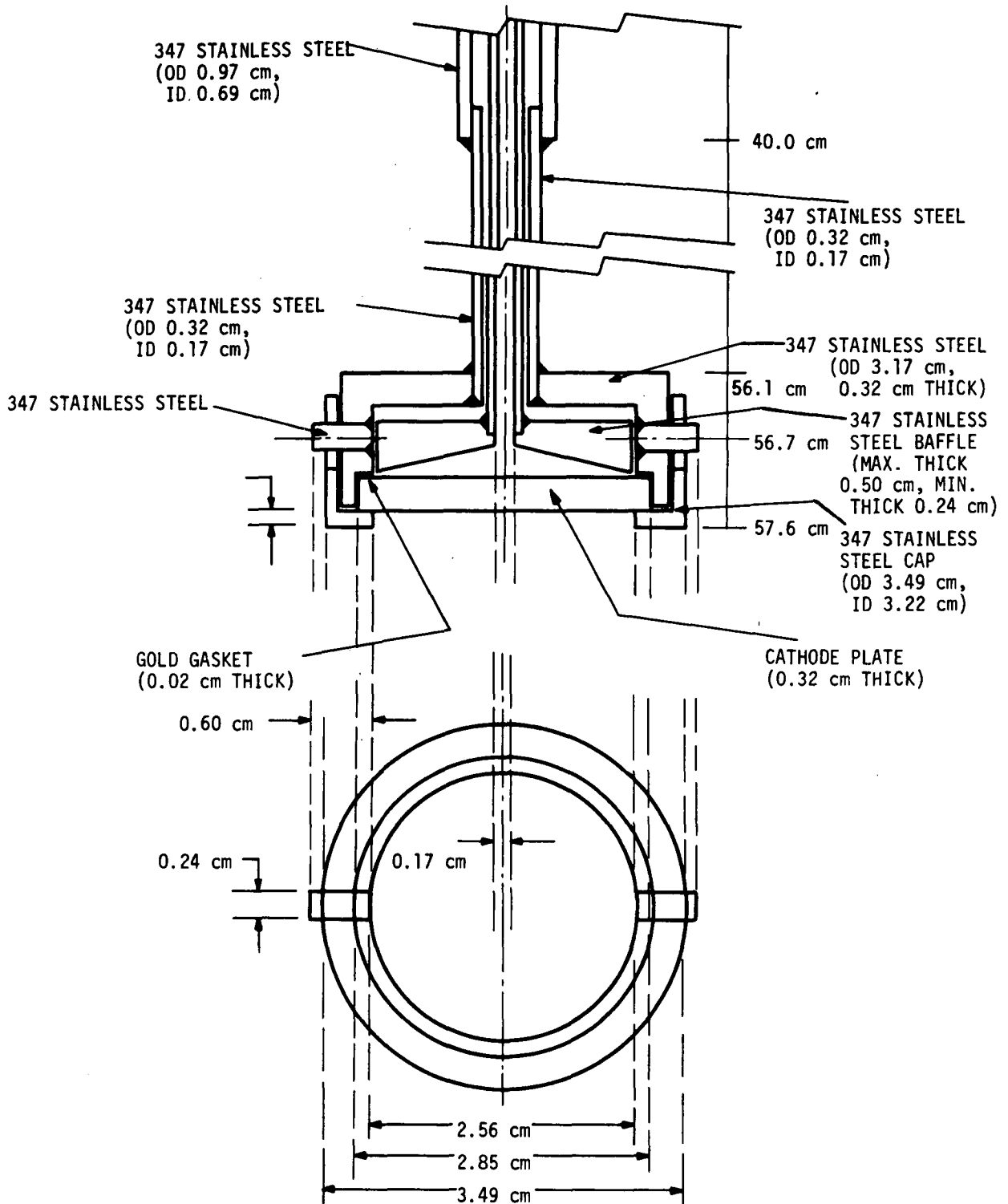


Fig. D.1b. Cathode, Lower Part (Vertical Section and Horizontal Section Through Cathode Holder)

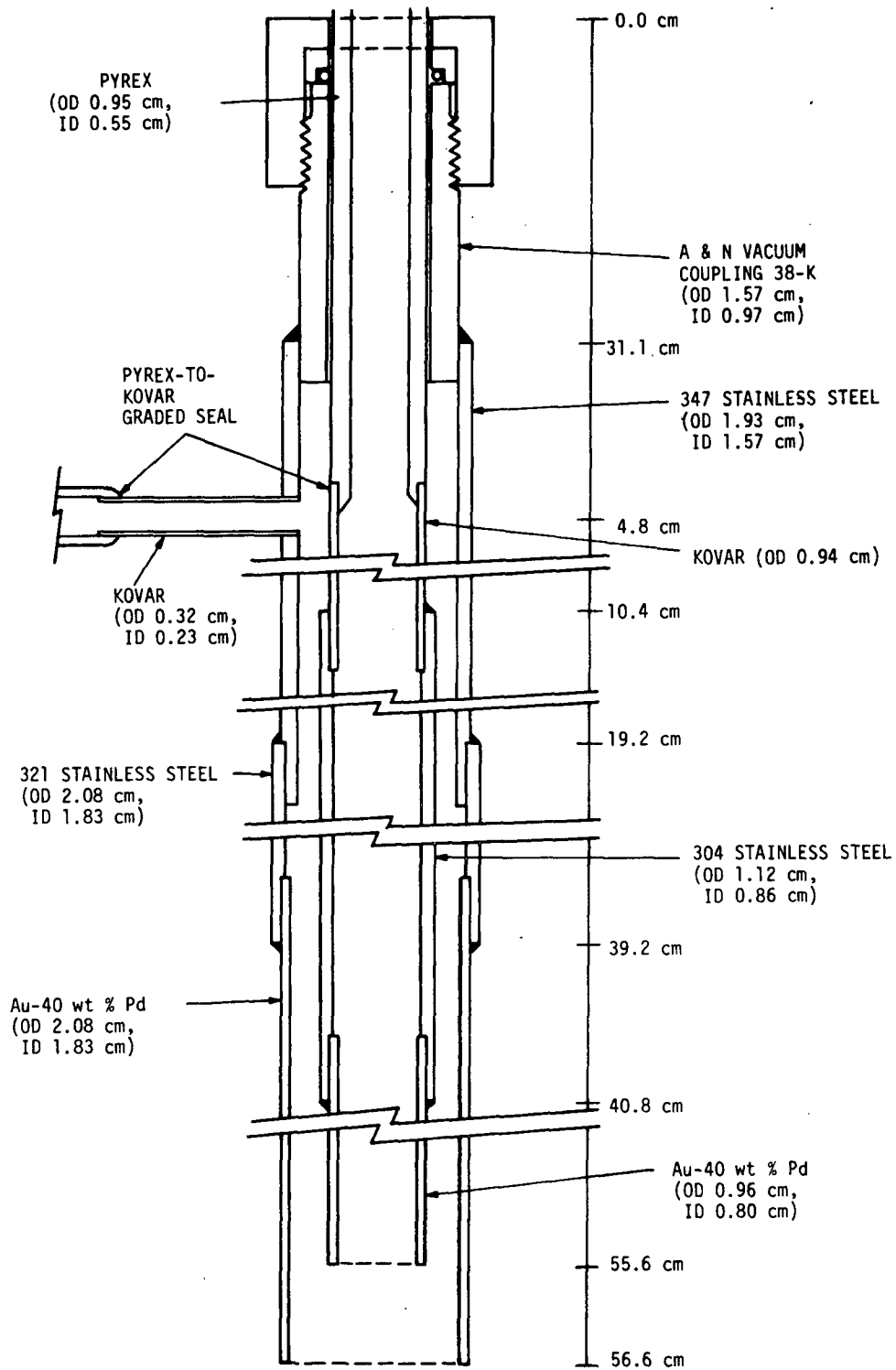


Fig. D.2. Anode (Vertical Section)

REFERENCES

1. J. R. Aylward, C. R. Russel, S. Russel, and J. I. Smith, "Research and Development Program for a Combined Carbon Dioxide Removal and Reduction System," Contract No. NAS1-4154, Final Report, May 1971 (NASA Contractor Report No. 111885, SVH SER 5863).
2. J. O'M. Bockris, A. Calandra, and C. Solomons, "Research and Development Program for a Combined Carbon Dioxide Removal and Reduction System--Supplement 1," Contract No. NAS1-4154, Final Report--Phase IIA, HSER 4908, Supplement 1, February 1969 (NASA Contractor Report No. 66519A), pp.43, 47.
3. Ref. 1, pp. 26, 28.
4. G. J. Janz and A. Conte, "Potentiostatic Polarization Studies in Fused Carbonates," *Electrochim. Acta* 9, 1269-1287 (1964).
5. N. M. Beskorovainyi and V. K. Ivanov, "Mechanism Underlying the Corrosion of Carbon Steels in Lithium," in *High Purity Metals and Alloys*, V. S. Emel'yanov and A. I. Evstyukhin, Eds. (Transl.) Consultants Bureau, New York (1967), pp. 121-129.
6. M. D. Ingram and G. J. Janz, "The Thermodynamics of Corrosion in Molten Carbonates; Application of E/P_{CO_2} Diagrams," *Electrochim. Acta* 10, 783-792 (1965).
7. Ref. 1, p. 26.
8. Ref. 1, p. 27 (Table I).
9. JANAF *Thermochemical Tables*, The Dow Chemical Co., Midland, Michigan (Dec. 31, 1960).
10. N. M. Beskorovainyi, V. K. Ivanov, and M. T. Zuev, "Behavior of Carbon in Systems of the Metal-Molten Lithium-Carbon Type," *High Purity Metals and Alloys*, V. S. Emel'yanov and A. I. Evstyukhin, Eds., Consultants Bureau, New York (1967).
11. G. K. Johnson, E. H. Van Deventer, J. P. Ackerman, Jr., W. N. Hubbard, D. W. Osborne, and H. W. Flotow, "Enthalpy of Formation of Disodium Acetylides and of Monosodium Acetylides at 298.15°K, Heat Capacity of Disodium Acetylides from 5 to 350°K, and Some Derived Thermodynamic Properties," *Journal of Chemical Thermodynamics*, 5 (1973) 57-71.
12. T. Ya. Kosolapova, *Carbides*, Moscow (1968) transl: Plenum Press, New York (1971).
13. C. E. Wicks and F. E. Block, "Thermodynamic Properties of 65 Elements - Their Oxides, Halides, Carbides, and Nitrides," Bureau of Mines Bulletin 605, U.S. Government Printing Office, Washington (1963), p. 28.
14. V. B. Parker, D. D. Wagman, and W. H. Evans, "Selected Values of Chemical Thermodynamic Properties," National Bureau of Standards Technical Note 270-6, U.S. Government Printing Office, Washington, D. C. (November 1971).
15. B. E. Conway, J. O'M. Bockris: "Electrolytic Hydrogen Evolution Kinetics and Its Relation to the Electronic and Adsorptive Properties of the Metal", *J. Chem. Physics* 26, 532-541 (1957).
16. J. M. Prausnitz: "Molecular Thermodynamics of Fluid-Phase Equilibria," Englewood Cliffs, N. J. (1969), p. 126ff.